Recent results from the Pierre Auger Observatory

Isabelle Lhenry-Yvon for the Pierre Auger Collaboration
IPN Orsay, Université Paris XI, CNRS/IN2P3

RICAP-14, Noto, September 30th-October 3rd

Outline

The Pierre Auger Observatory

Science case and characteristics

Results, towards the understanding of UHECR's

Spectrum,

Mass composition (hadronic)

Anisotropy

Summary and future

OPEN QUESTIONS ABOUT UHECR

- What is their nature ?
- Where to they come from ?
- How are they produced ?
- Is there a maximum limit to their energy?
- How do they propagate ?
- What can they tell us about particle physics ?

The Pierre Auger Observatory in Argentina

Surface detectors

1680 Cherenkov stations
1.5 Km spaced on a hexagonal grid
Can detect shower up to 90°
100% duty cycle

Fluorescence detectors

4 building with 6 telescopes each
Telescope f.o.v. 30 x 30
~15 % duty cycle

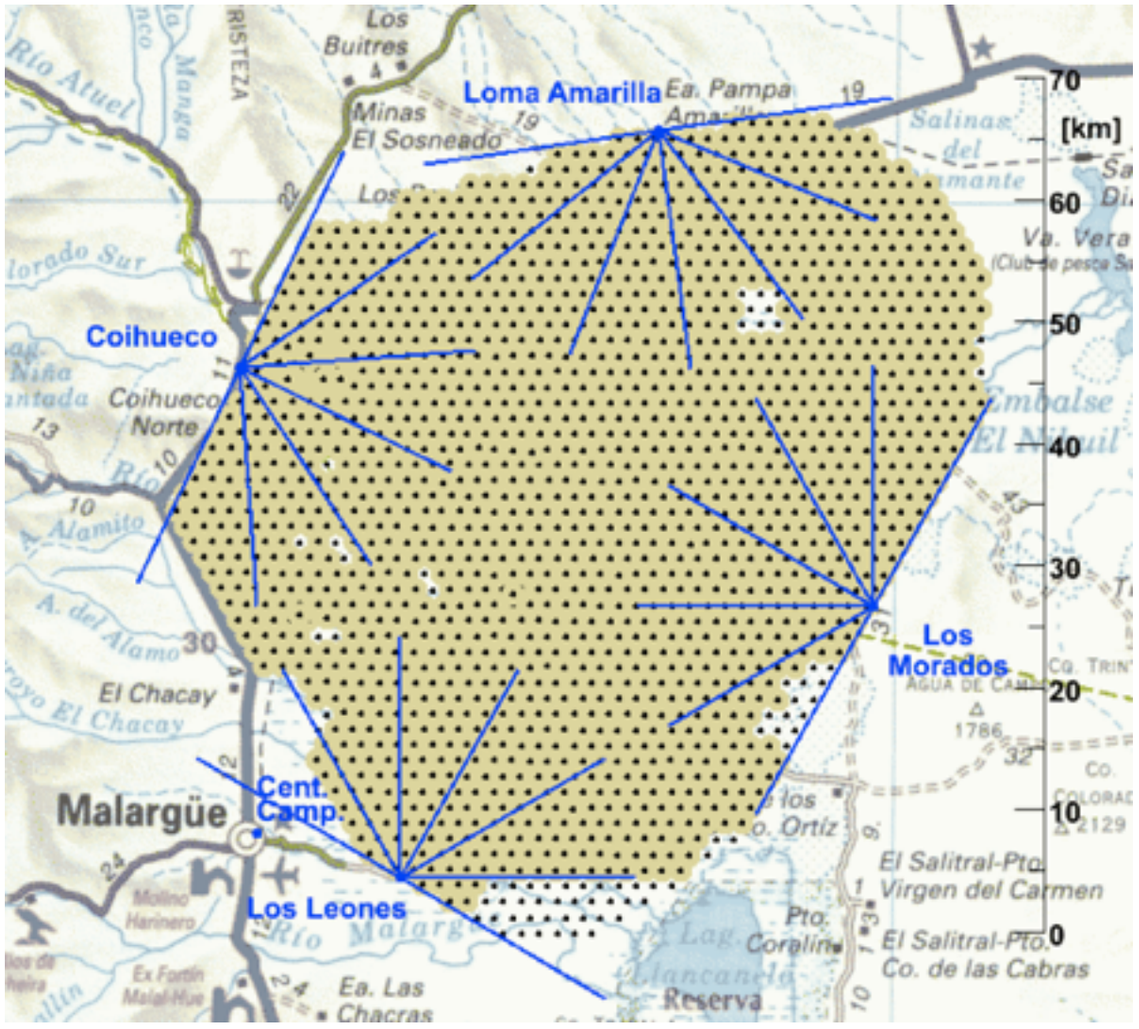

Completed in 2008
Progressive data taking starting in 2004

Aiming at understanding the origin of Ultra High Energy Cosmic Rays, the PAO associates the widest detection surface (3000 km^2) together with the highest precision ever achieved

Auger Hybrid concept: more than 2 detectors !

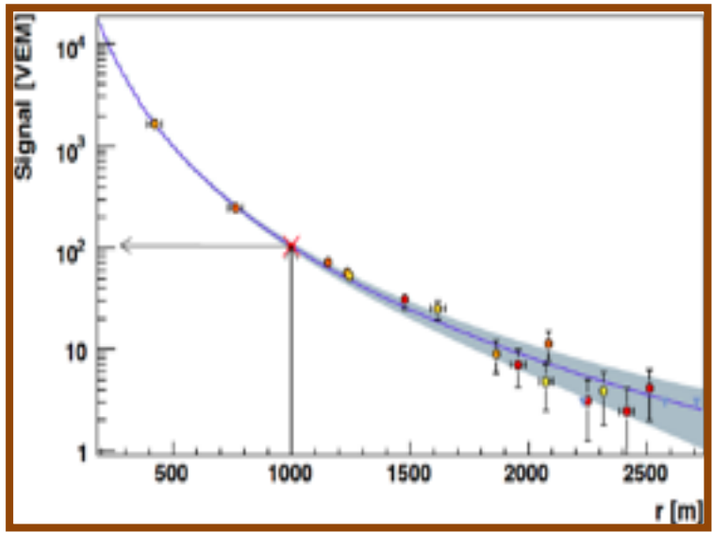

Lateral profile by SD

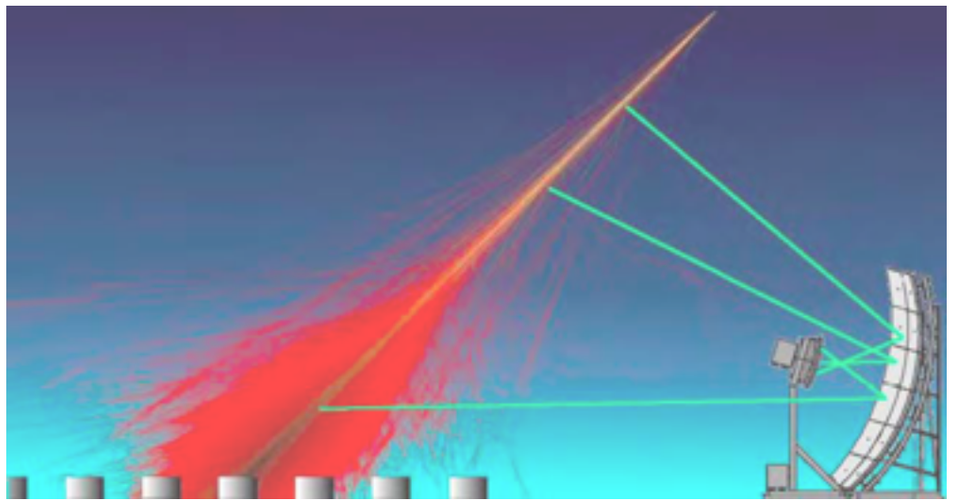

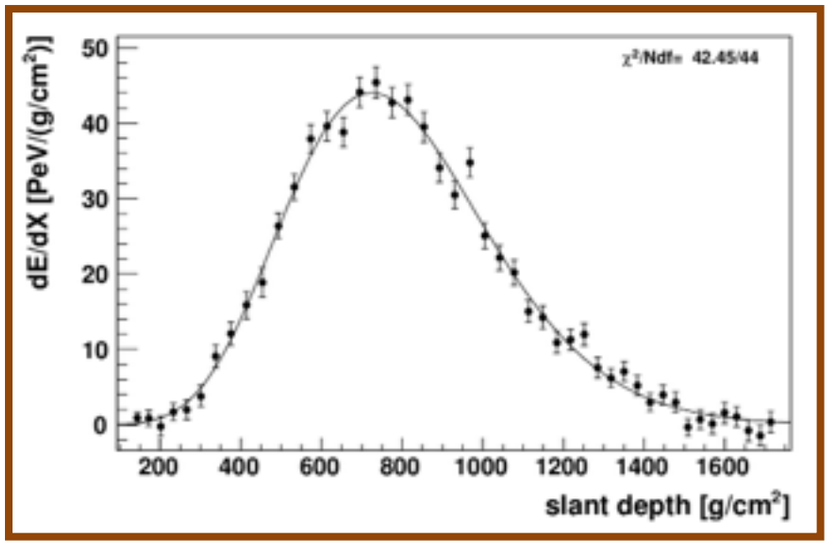

Longitudinal profile by FD

SD provides:
- Huge aperture (100% duty cycle) easily calculable
- Large angular acceptance (showers up to 80°)
- Robust detectors
- Good angular resolution

FD provides:
- Fluorescence light emitted in proportion to energy deposit: -> Near calorimetric energy measurements
- A direct view of shower maximum (composition)
- Precise directions (hybrid method).
- But duty cycle is only 10-15%

Optimisation of Auger's hybrid data

- FD calibrates SD energy scale that is used on the large statistic of SD events
- minimise (when possible) use of simulations in the production of key scientific output (SD energy spectrum, composition(~ minimal use))
- Various cross-check (directions, energy thresholds…)
- Use of different data sets

Present status of the Pierre Auger Observatory

LOW ENERGY EXTENSION (10^{17} - 3 10^{18} eV)

HEAT

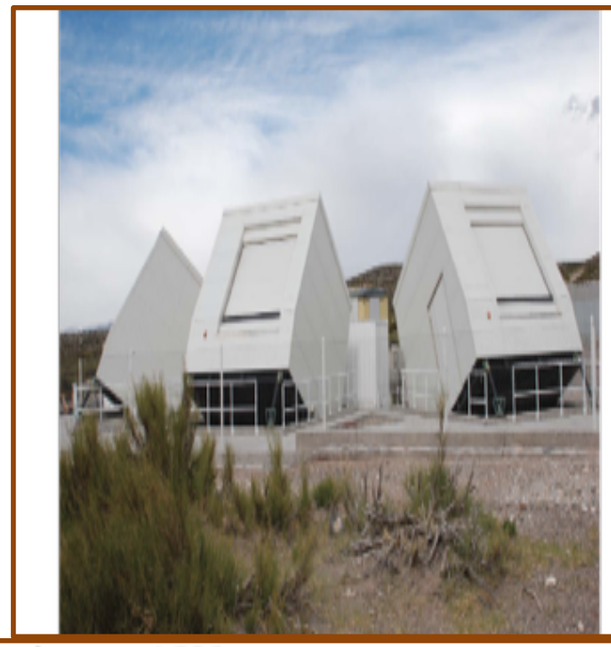

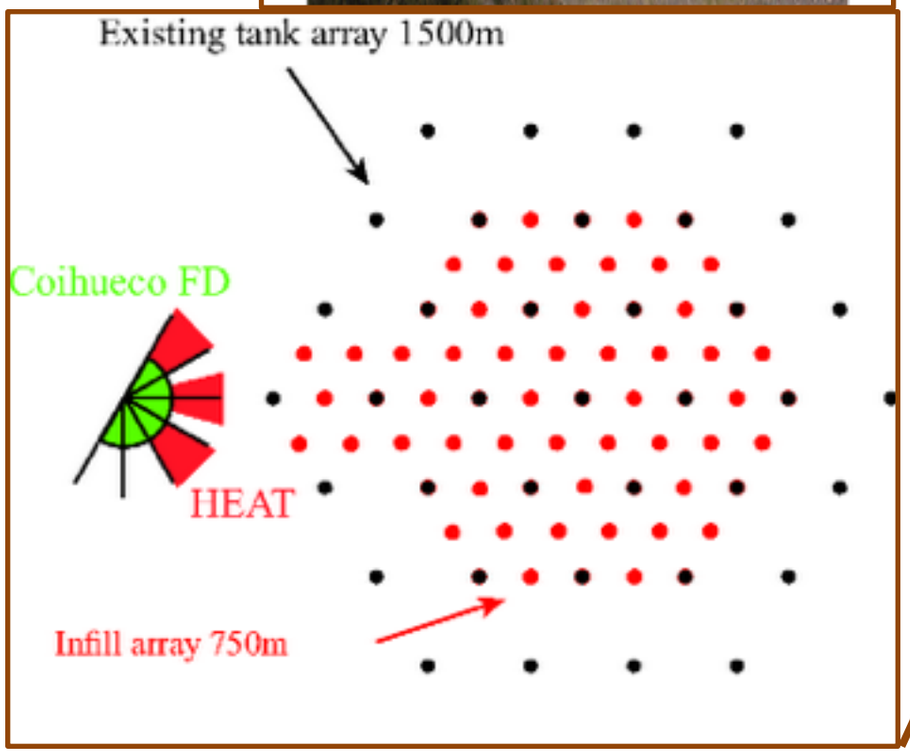

750 m ARRAY

1500 m ARRAY

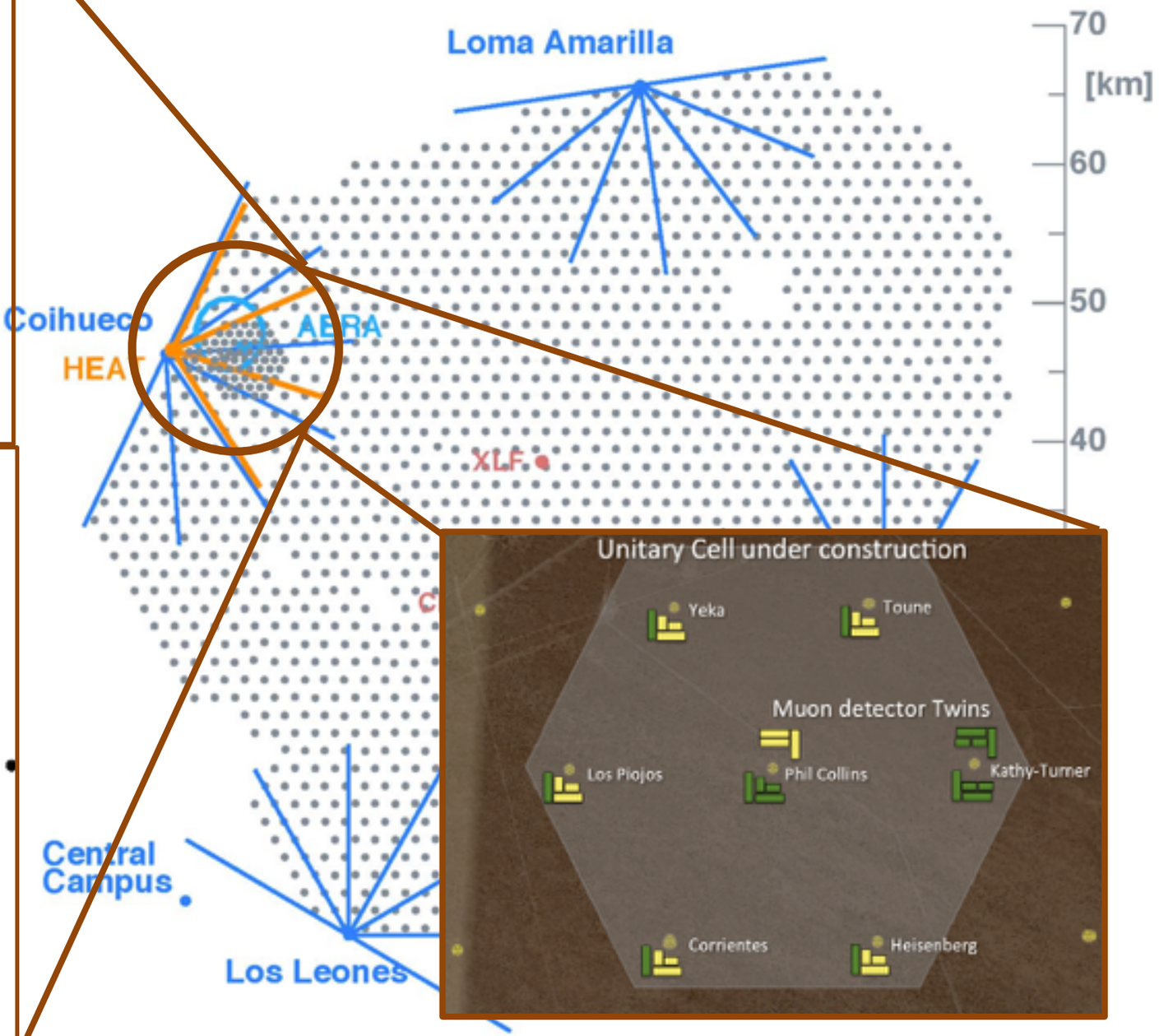

AMIGA MUON COUNTERS

AUGER DATA SETS

SD 1500 m, $\theta < 60°$

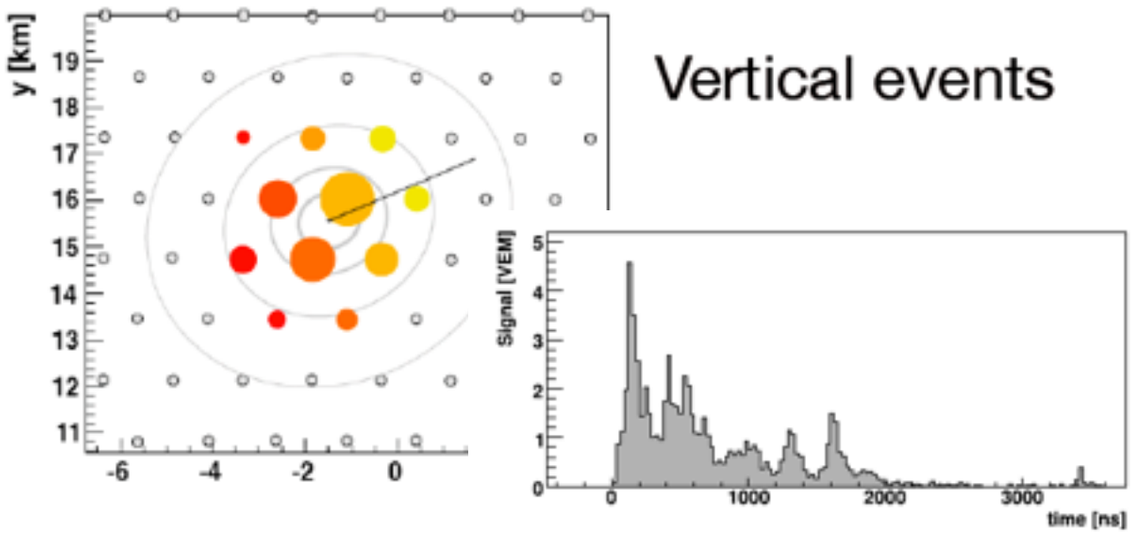

Vertical events

SD 750 m, $\theta < 55°$

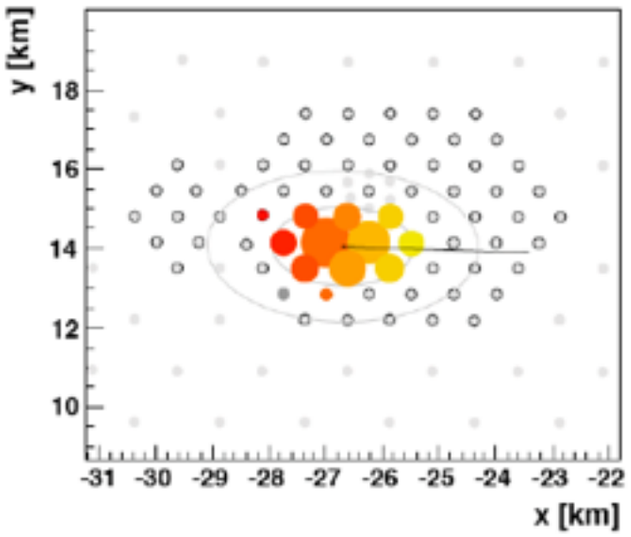

750m events

SD 1500 m, $62° < \theta < 80°$

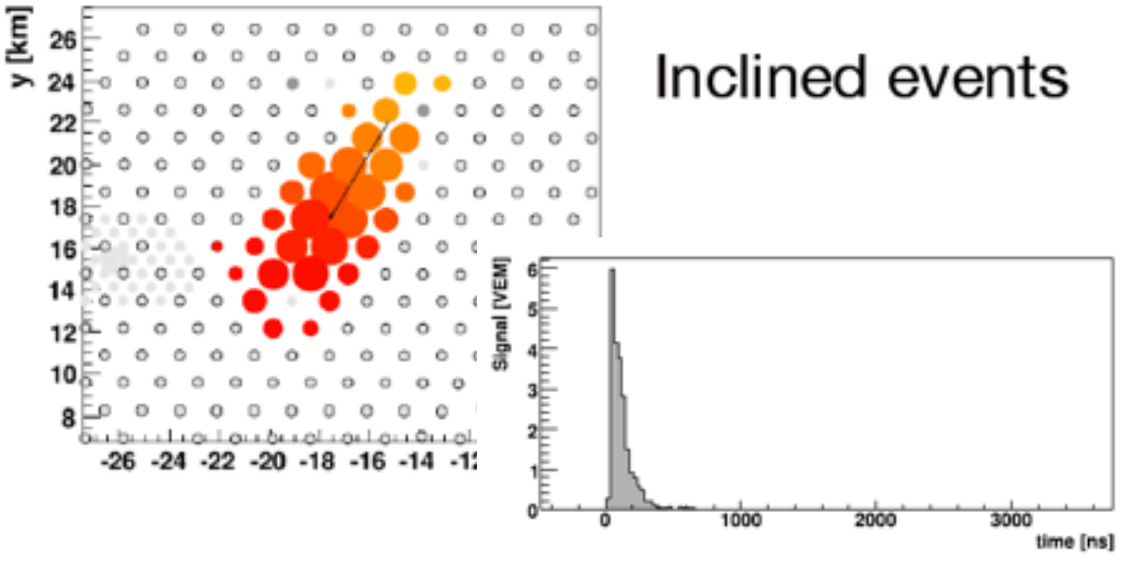

Inclined events

Hybrid(FD + 1 SD), $\theta < 60°$

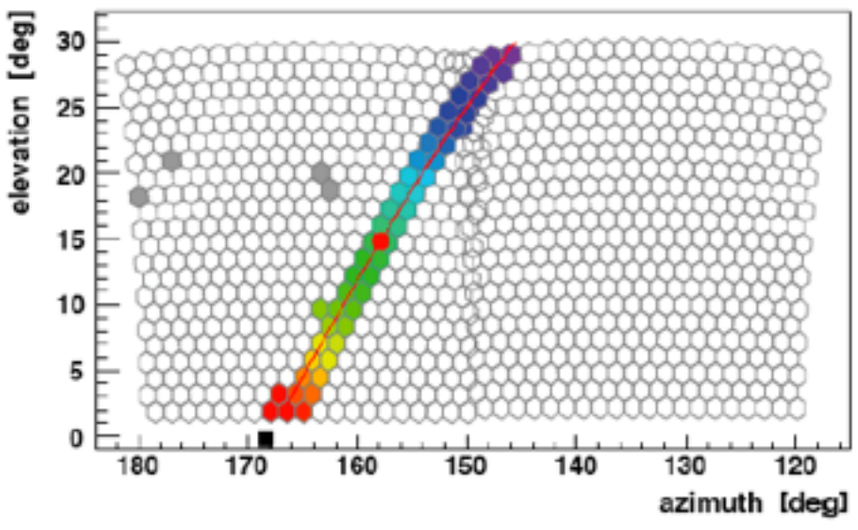

Hybrid events

SPECTRUM

ENERGY RECONSTRUCTION OF AUGER EVENTS

SD estimators calibrated with FD energy

SD vertical ($\theta < 60°$)

Energy estimator S(1000):

Signal at 1000 m from lateral profile

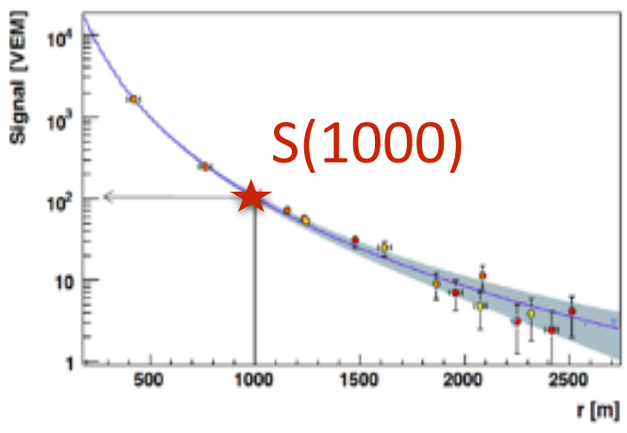

S(1000) is θ dependent due to attenuation in atmosphere

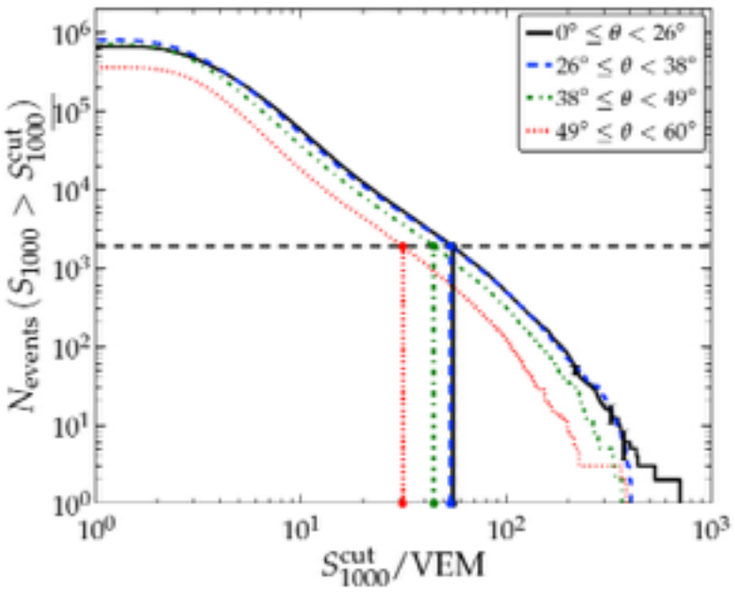

Use of Constant Intensity Cut (CIC) to have a zenithal angle independent estimator S38

ABOUT Constant Intensity Cut

Attenuation curves inferred from data only

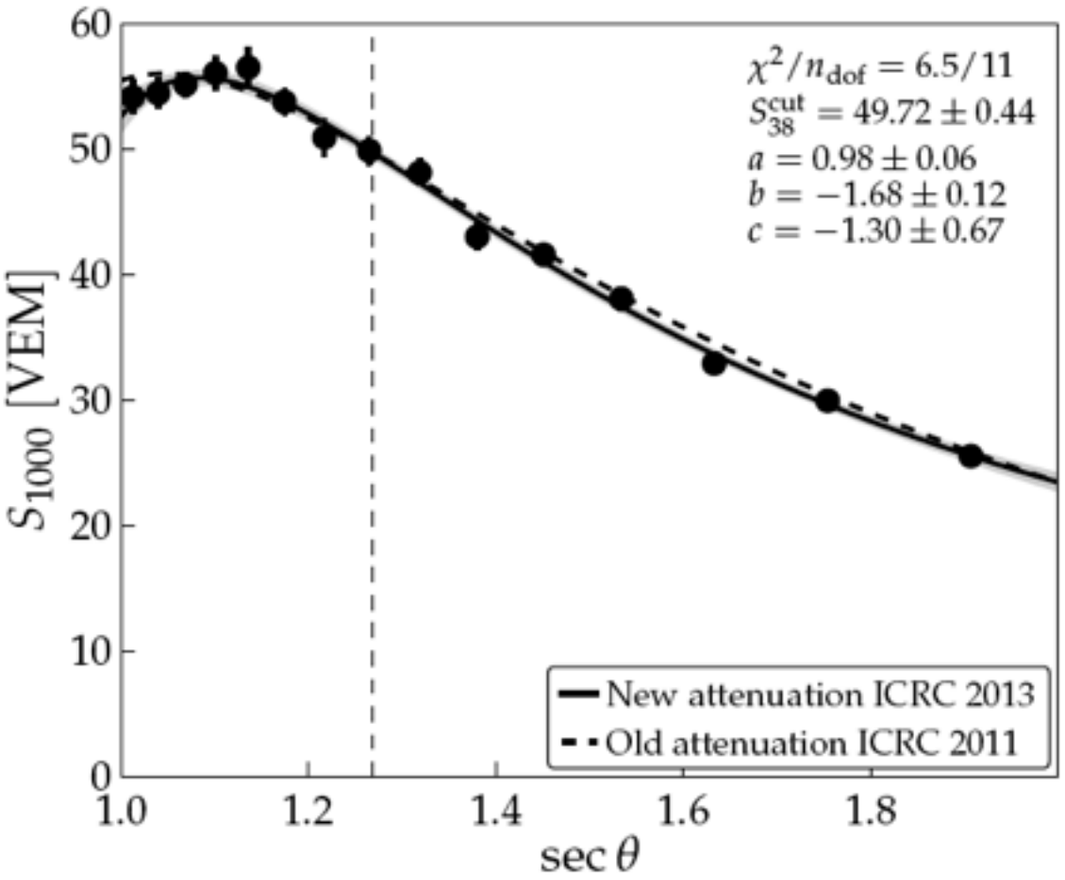

$$S_{38} = S(1000)/\mathrm{CIC}(\theta)$$

Zenithal angle independent estimator

$$\mathrm{CIC}(\theta) = 1 + ax + bx^2 + cx^3 \quad (x = \cos^2\theta - \cos^2 38^\circ)$$

No energy dependence above ≈ 20VEM ≈ 6 EeV

ENERGY RECONSTRUCTION OF AUGER EVENTS

SD vertical (θ < 60°)

Energy estimator S(1000):

Signal at 1000 m from lateral profile

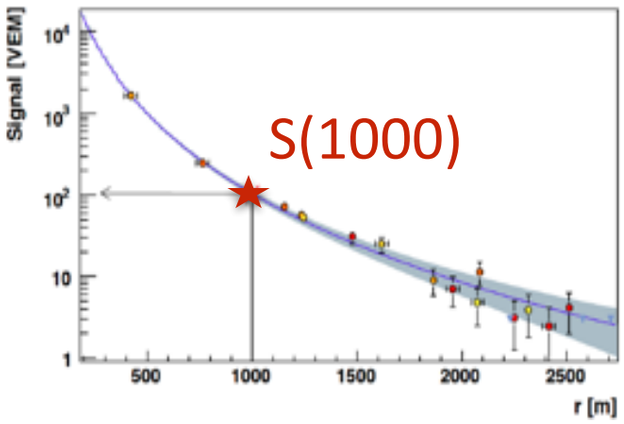

S(1000) is θ dependent due to attenuation in atmosphere

-> use of Constant Intensity Cut (CIC)

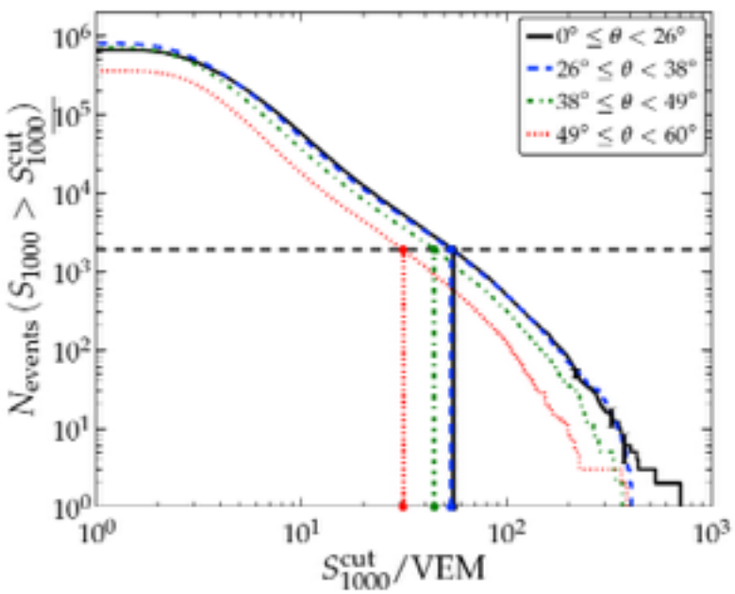

Conversion S(1000)->S_{38}

In case of SD 750m array: S(450) S35

SD horizontal al (62 < θ < 80°)

Energy estimator : N_{19}

N_{19}: relative number of muons at ground w.r.t. the density of muons of the reference distribution:

$$\rho_\mu = N_{19}\rho_{\mu,19}(x, y, \theta, \phi)$$

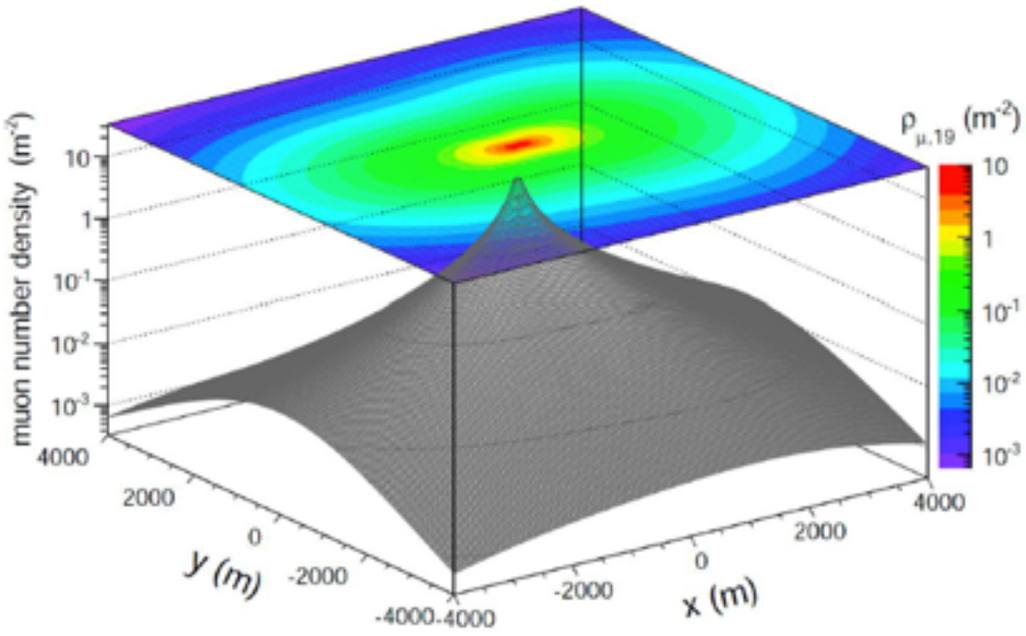

Example of $\rho_{\mu,19}$ for proton showers at θ=80°, ϕ=0° and core at (x,y) = (0,0)

$\rho_{\mu,19}$ reference profile from parameterization of muon density at ground (10^{19} eV p QGSJetII-03)

N_{19} is not θ dependent (already included in $\rho_{\mu,19}$)

Calibration of AUGER data sets

For each SD data , the energy estimator is calibrated with FD energy with hybrid data set

Cross correlation of the SD energy estimators (S) with the FD energy

$$E_{FD} = A * S^B$$

- SD 1500 m:
  $A = (0.190 \pm 0.005)\,\mathrm{EeV}$
  $B = 1.025 \pm 0.007$
- SD inclined:
  $A = (5.61 \pm 0.1)\,\mathrm{EeV}$
  $B = 0.985 \pm 0.02$
- SD 750 m:
  $A = (12.1 \pm 0.7)\,\mathrm{PeV}$
  $B = 1.03 \pm 0.02$

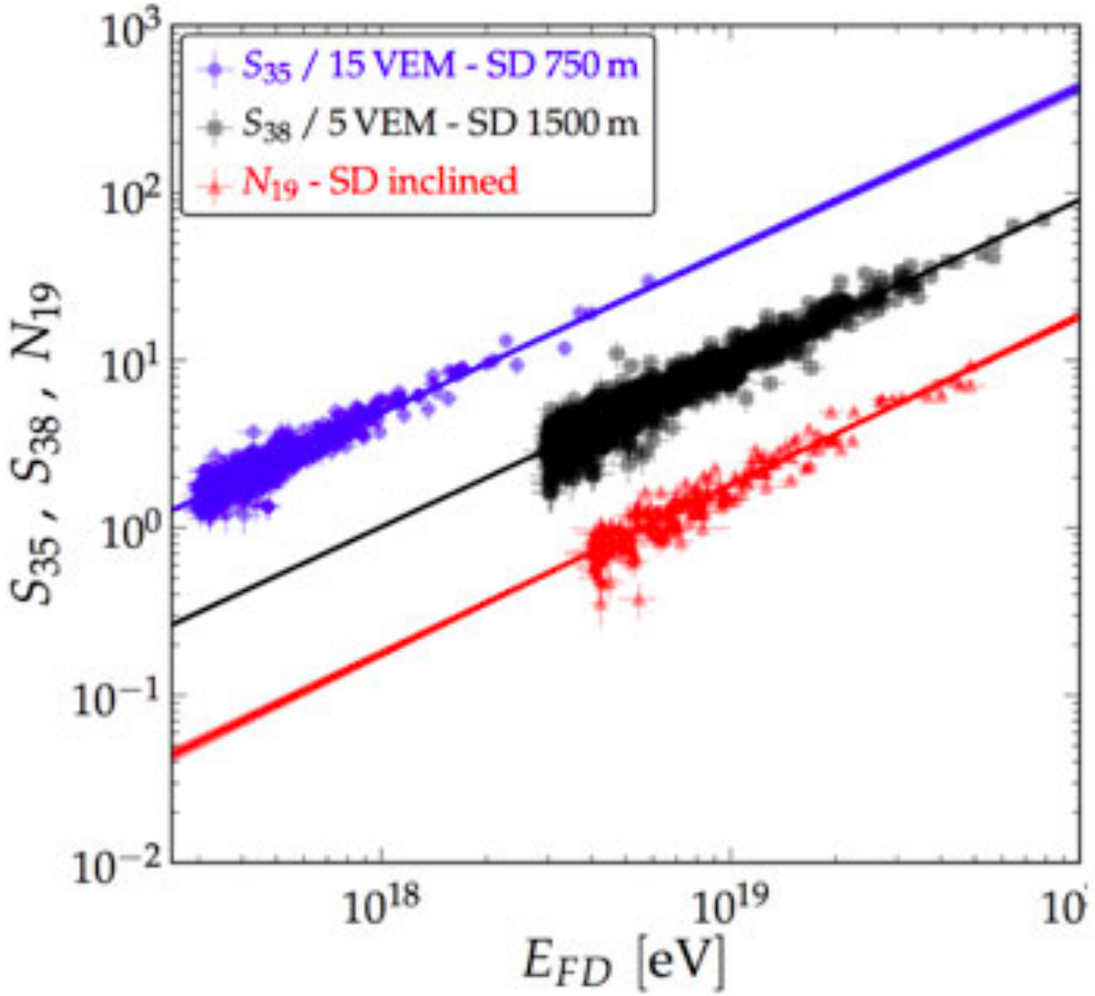

SD energies do not rely on MC

New Energy scale from FD Energy

Changes in : Atmosphere, fluorescence yield, invisible energy, FD calibration
Longitudinal profile fit (at ICRC2013)

at 10^{18} eV

Absolute fluorescence yield	**-8.2%**
New opt. eff.	4.3%
Calibr. database update	3.5%
Sub total (FD cal.)	**7.8%**
Likelihood fit of dE/dX	2.2%
Folding with point. spr. func.	9.4%
Sub total (FD prof. rec.)	**11.6%**
Invisible energy	**4.4%**
Total	**15.6%**

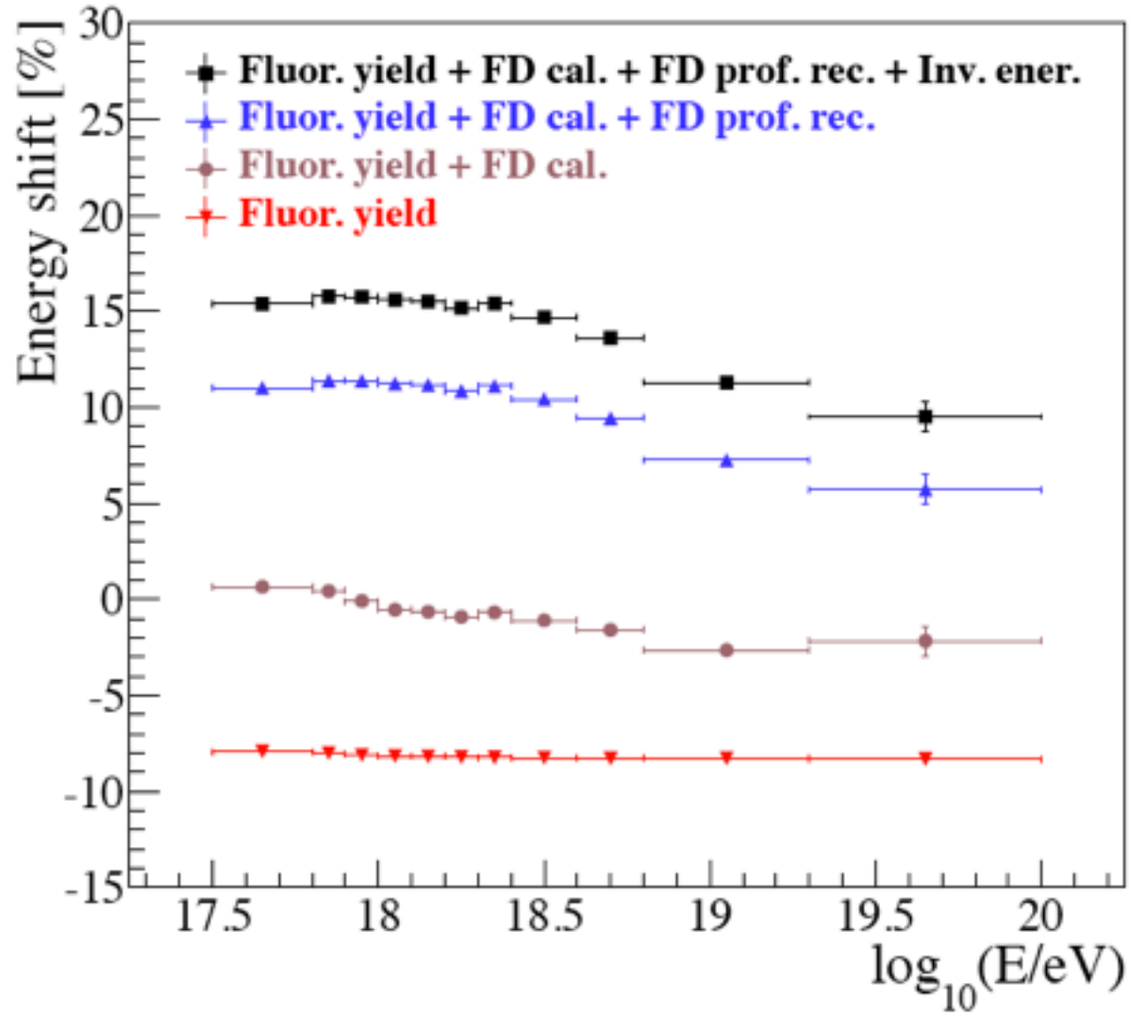

Still compatible with former uncertainty (22%)

Systematic uncertainties on the SD energy scale

Absolute fluorescence yield	3.4%
Fluores. spectrum and quenching param.	1.1%
Sub total (Fluorescence Yield)	**3.6%**
Aerosol optical depth	3% ÷ 6%
Aerosol phase function	1%
Wavelength dependence of aerosol scattering	0.5%
Atmospheric density profile	1%
Sub total (Atmosphere)	**3.4% ÷ 6.2%**
Absolute FD calibration	9%
Nightly relative calibration	2%
Optical efficiency	3.5%
Sub total (FD calibration)	**9.9%**
Folding with point spread function	5%
Multiple scattering model	1%
Simulation bias	2%
Constraints in the Gaisser-Hillas fit	3.5% ÷ 1%
Sub total (FD profile rec.)	**6.5% ÷ 5.6%**
Invisible energy	**3% ÷ 1.5%**
Statistical error of the SD calib. fit	**0.7% ÷ 1.8%**
Stability of the energy scale	**5%**
TOTAL	**14%**

FD uncertainties propagate to the SD energies

TOTAL ≈ 14%

~ independent of energy

AUGER DATA SETS EXPOSURE

Data selection for all SD data sets

only well contained events are selected

Hottest tank (or core for horizontal) must be surrounded by 6 active tanks

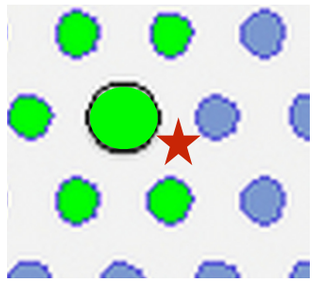

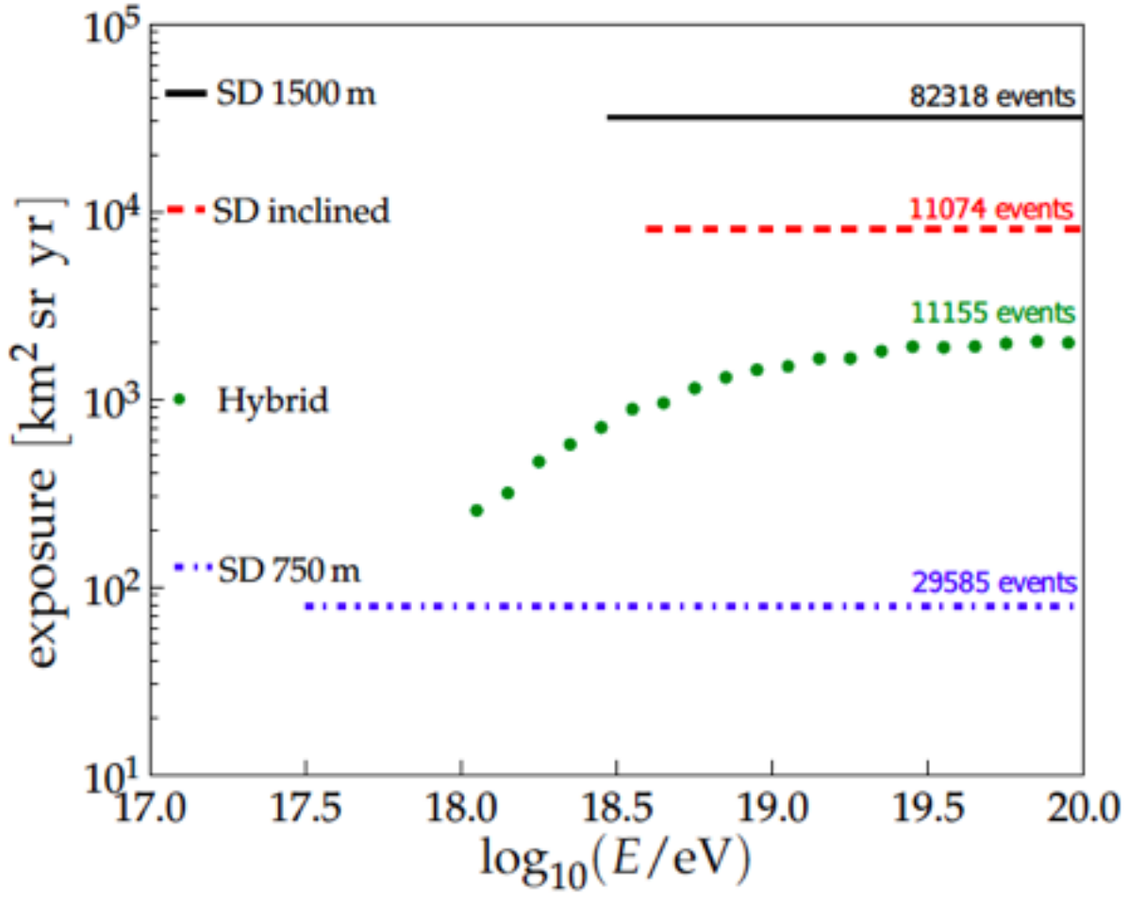

SD fully efficient above a certain threshold -> exposure is geometrical

- SD 1500 m > 3 10^{18} eV , θ < 60° — 31645 ± 950 km2 sr yr
- SD 750 m > 3 10^{17} eV , θ < 55° — 79 ± 4 km2 sr yr
- SD inclined > 4. 10^{18} eV, 60° <θ <80 ° — 8027 ± 240 km2 sr yr

+ Hybrid data : Exposure calculation with MC — 1496 ± 25 km2 sr yr

Energy spectrum

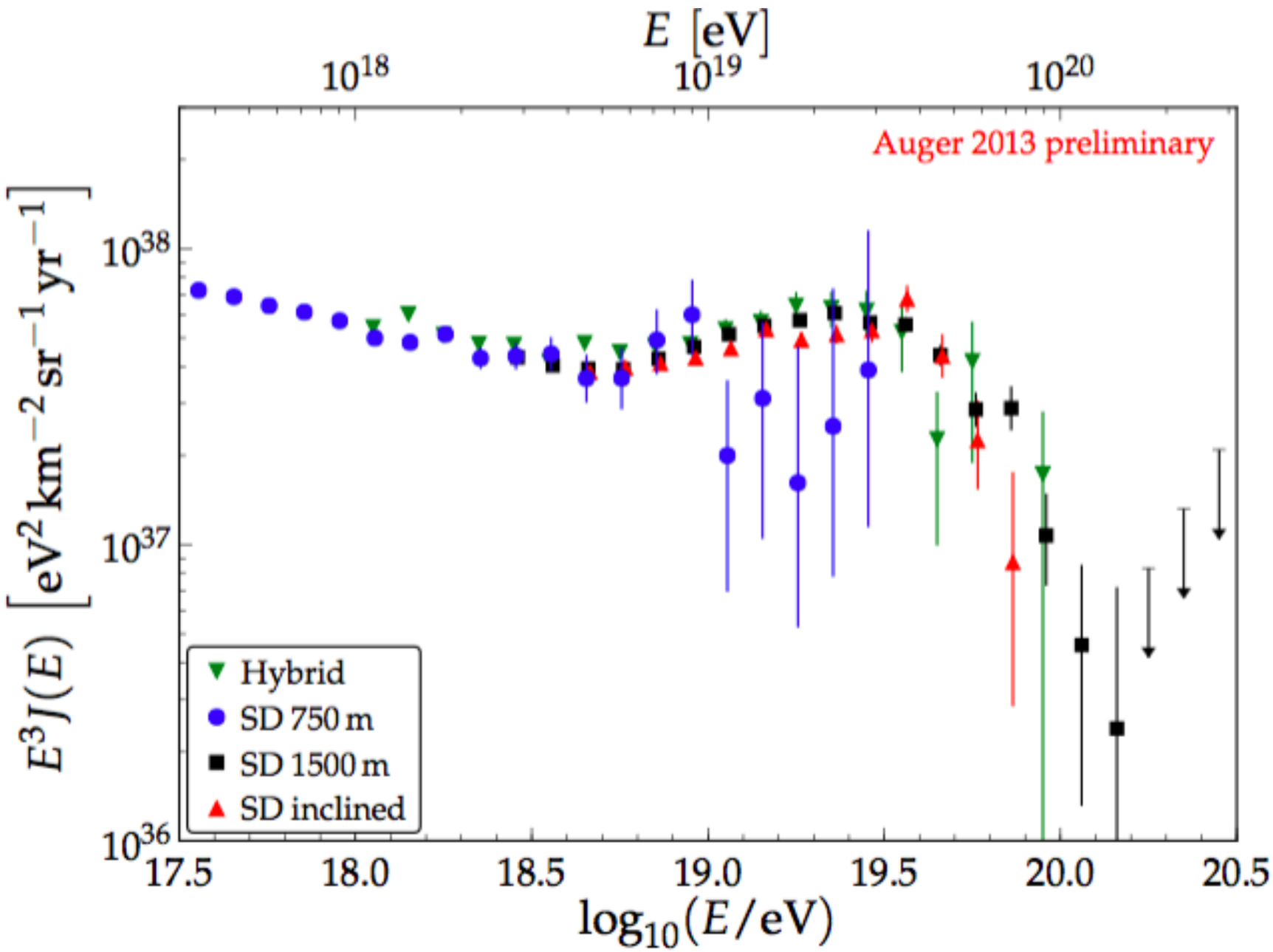

Energy spectrum

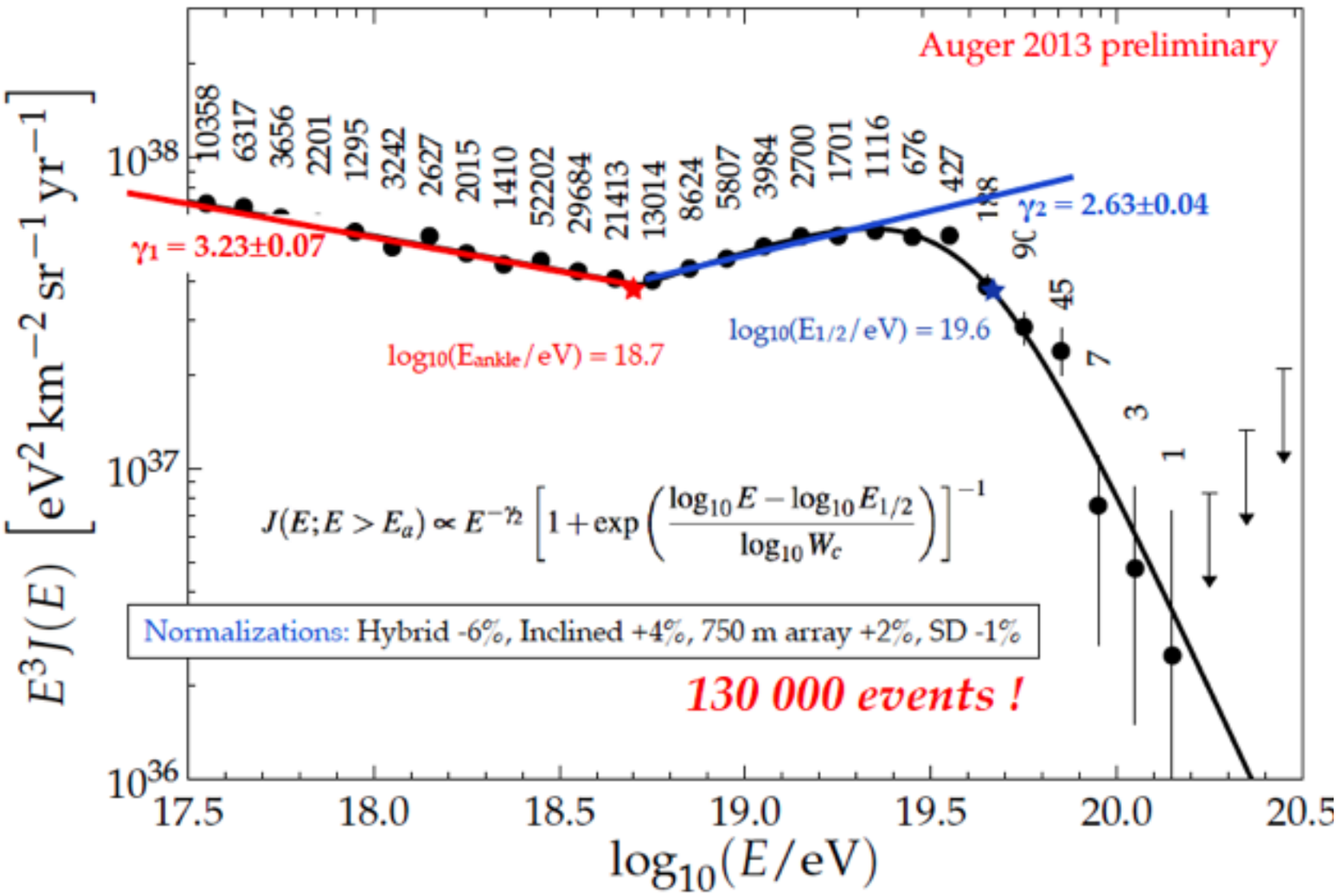

Is the galactic/extragalactic transition at the ankle ?

Is the cut off the GZK effect or a limit of the sources energies?

Fit function ➡ $$J(E;E>E_a) \propto E^{-\gamma_2}\left[1+\exp\left(\frac{\log_{10}E-\log_{10}E_{1/2}}{\log_{10}W_c}\right)\right]^{-1}$$

Spectrum and astrophysical scenarios

- Comparison to predictions from astrophysical scenarios
- Different primary and maximal energies (β-injection index =-2.35 (p), -2.3 (Fe))
- Models calculated with CRPropa and validated with SimProp

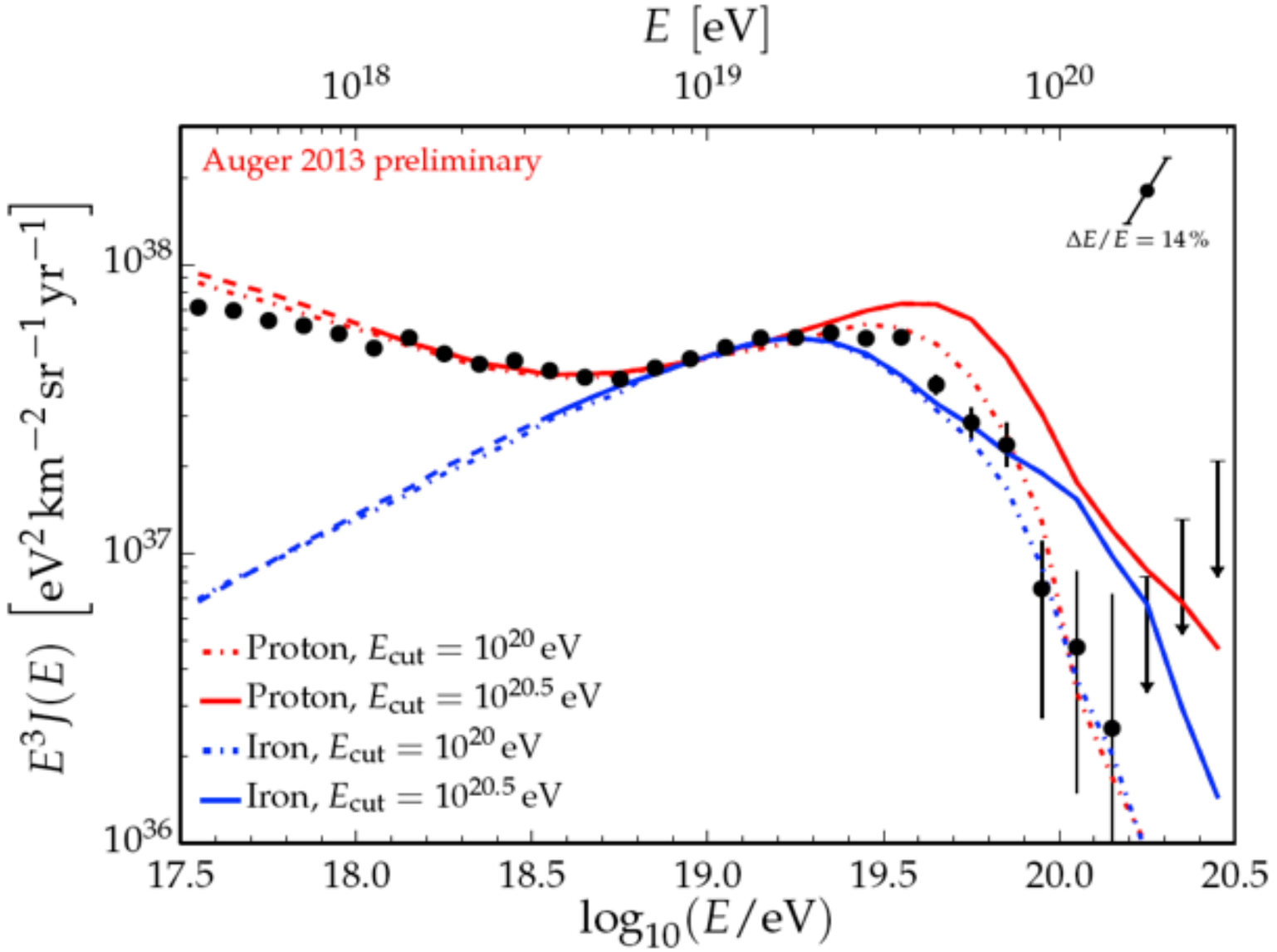

Spectrum alone is not enough to discriminate between scenarios

MASS COMPOSITION

Composition from FD longitudinal profile

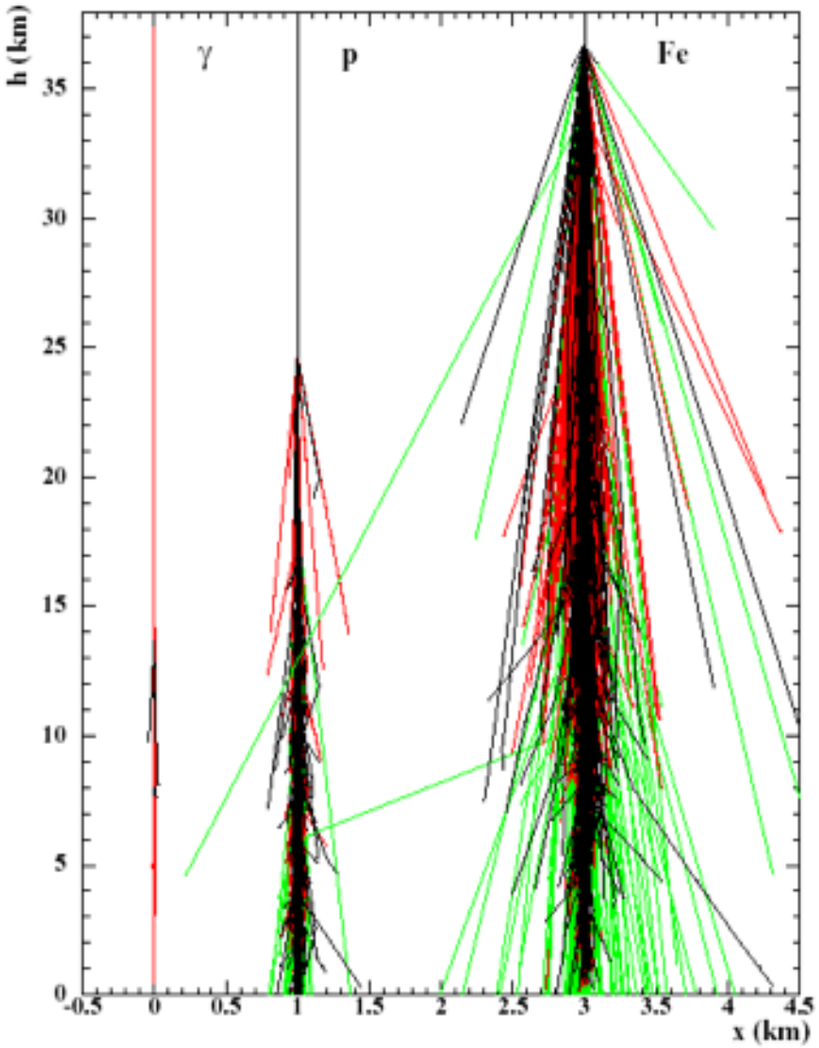

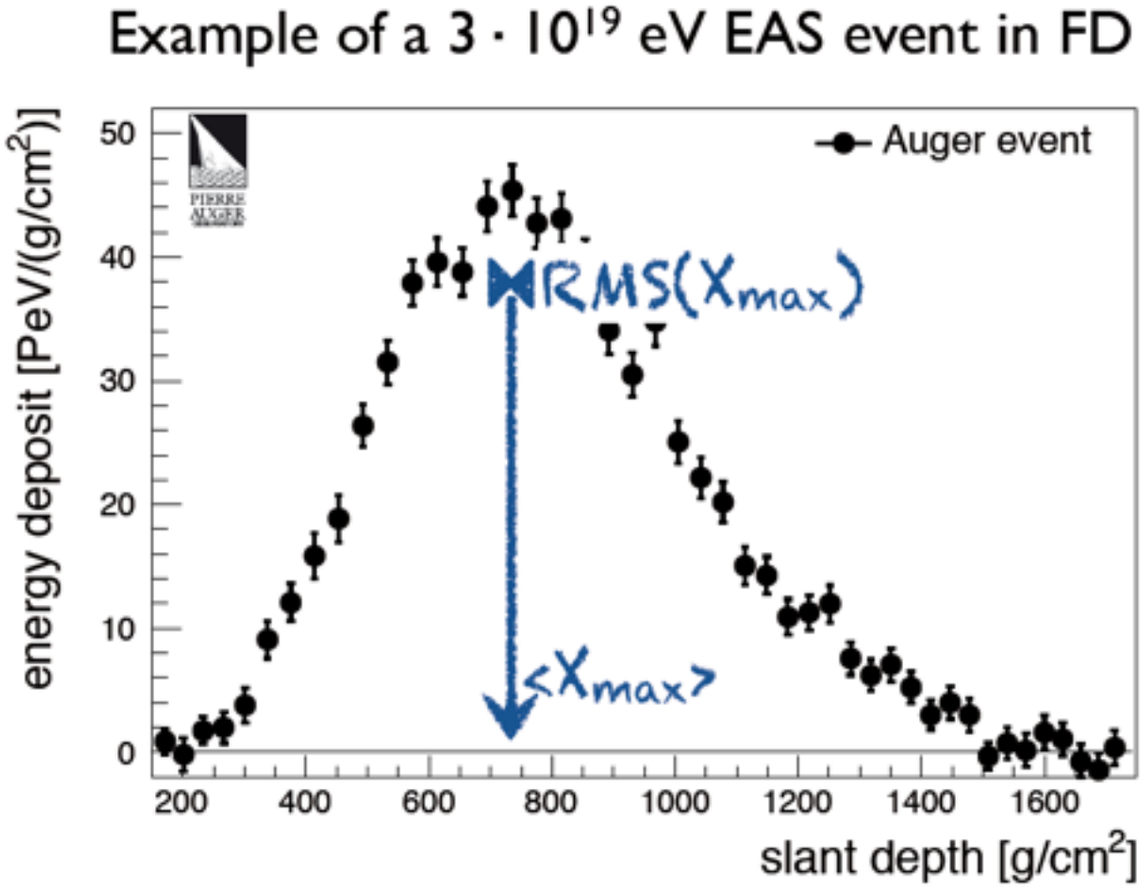

Fe shower develop higher in atmosphere
-> lower Xmax (~100g.cm-^{2} avrg)

Observables sensitive to composition:

- Depth of shower maximum (<Xmax>);
- Elongation rate (d<Xmax>/dlogE);
- RMS of Xmax distribution at fixed energy:

Data Selection

atmosphere and calibration

- good camera calibration constants
- require measured aerosol profile
- reject dust periods (VAOD@3km<0.1)
- cloud fraction < 25%

fiducial volume cuts

- surface detector trigger probability
- field of view
- minimum viewing angle > 20^o

quality selection

- hybrid geometry reconstruction
- Xmax observed
- expected σ(Xmax) < 40 g/cm^2
- reduced χ^2 of profile fit < 2.5

Good data taking conditions

Almost unbiased Xmax distributions

Good Xmax and Energy measurement

Mass composition - X_{max}

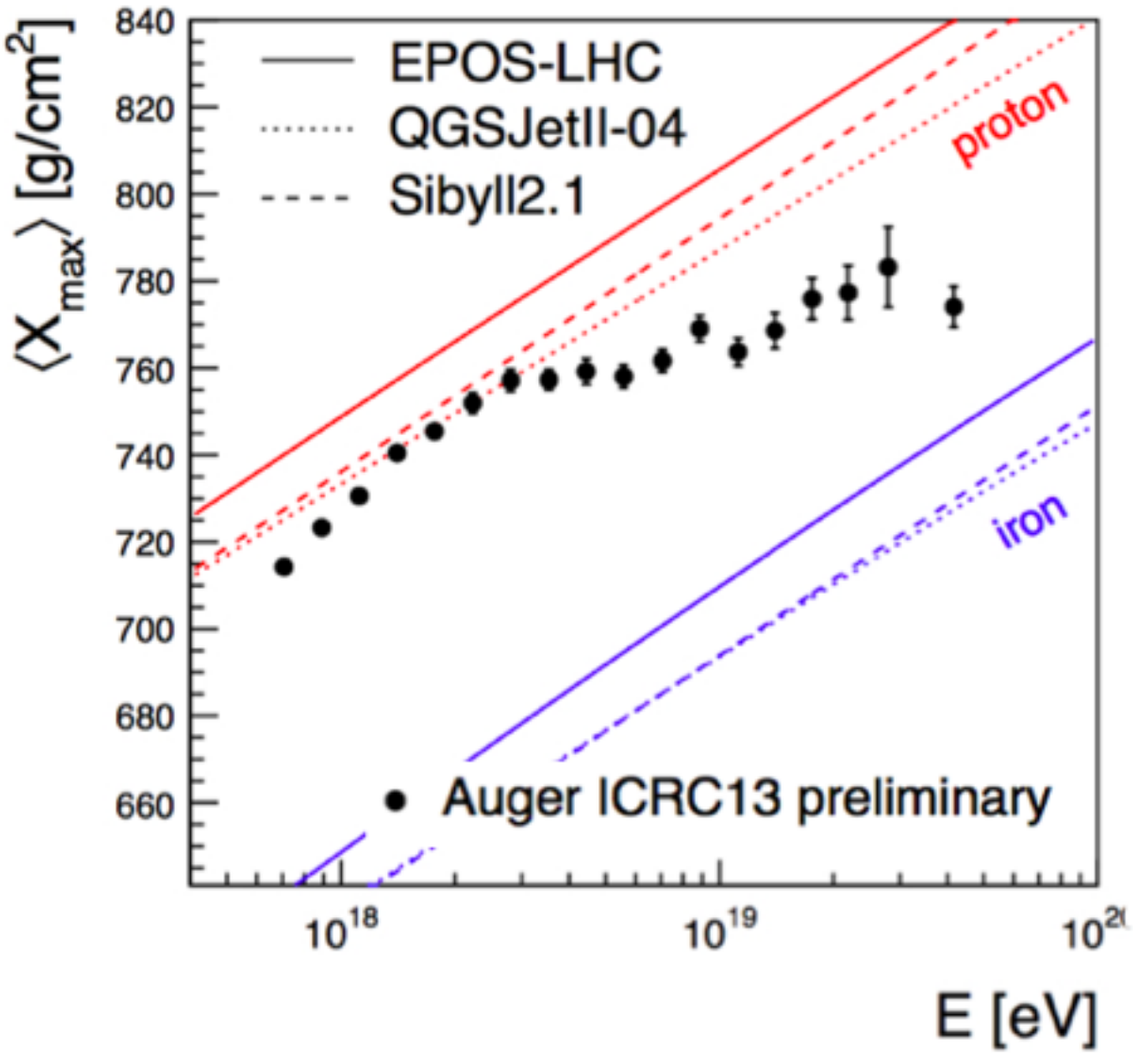

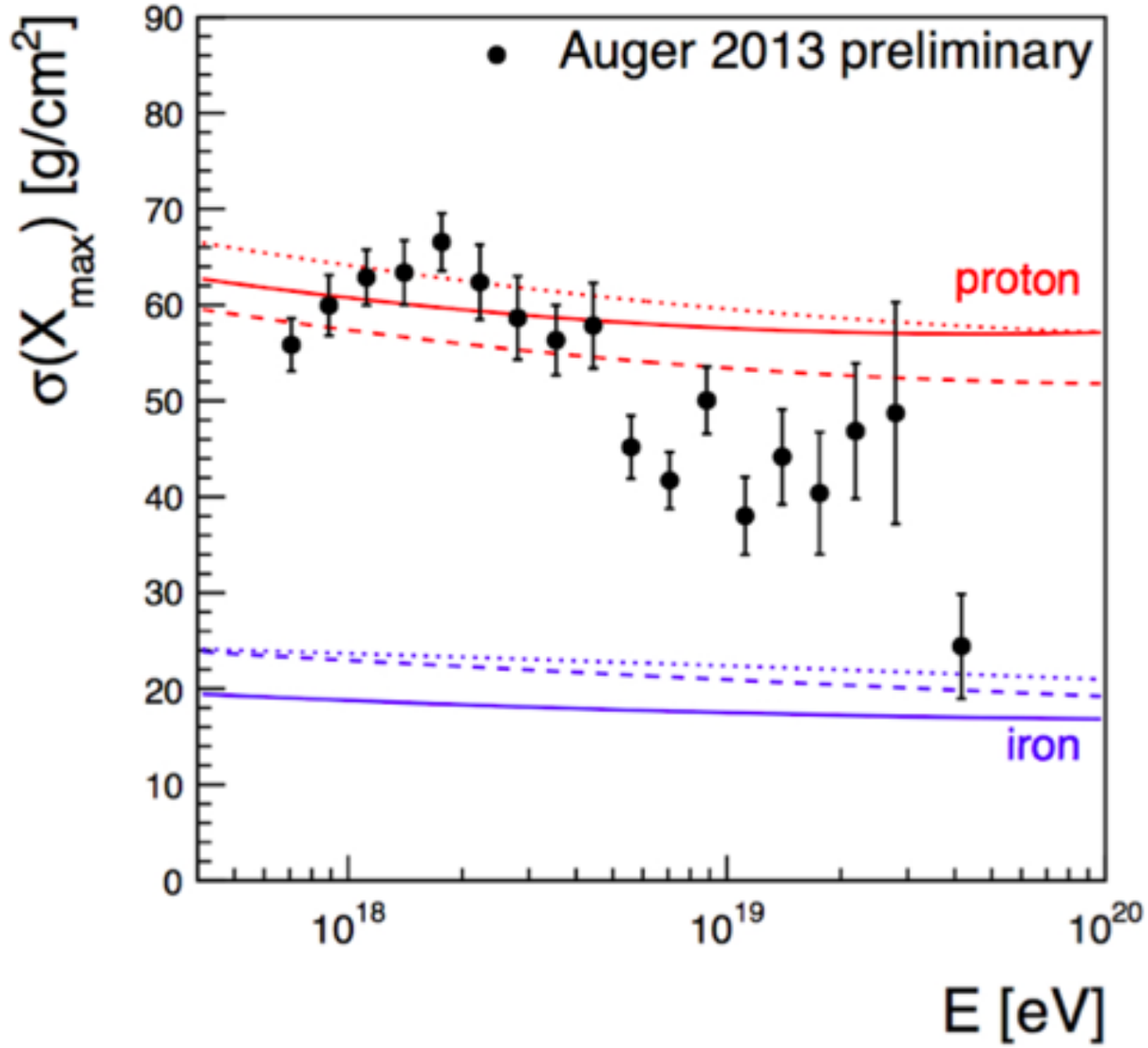

Change from a mixed/light composition to a heavier one

Mass composition - from Xmax to lnA

$$\langle X_{max}\rangle \simeq \langle X^{P}_{max}\rangle - D_p\langle \ln A\rangle \qquad \langle \ln A\rangle = \sum f_i \ln A_i$$
$$\sigma(X_{max})^2 \simeq \langle \sigma_i^2\rangle + D_p^2\,\sigma(\ln A)^2 \qquad \sigma(\ln A)^2 = \langle(\ln A)^2\rangle - \langle \ln A\rangle^2$$

D_p elongation rate <σi> mass-averaged fluctuations

lnA

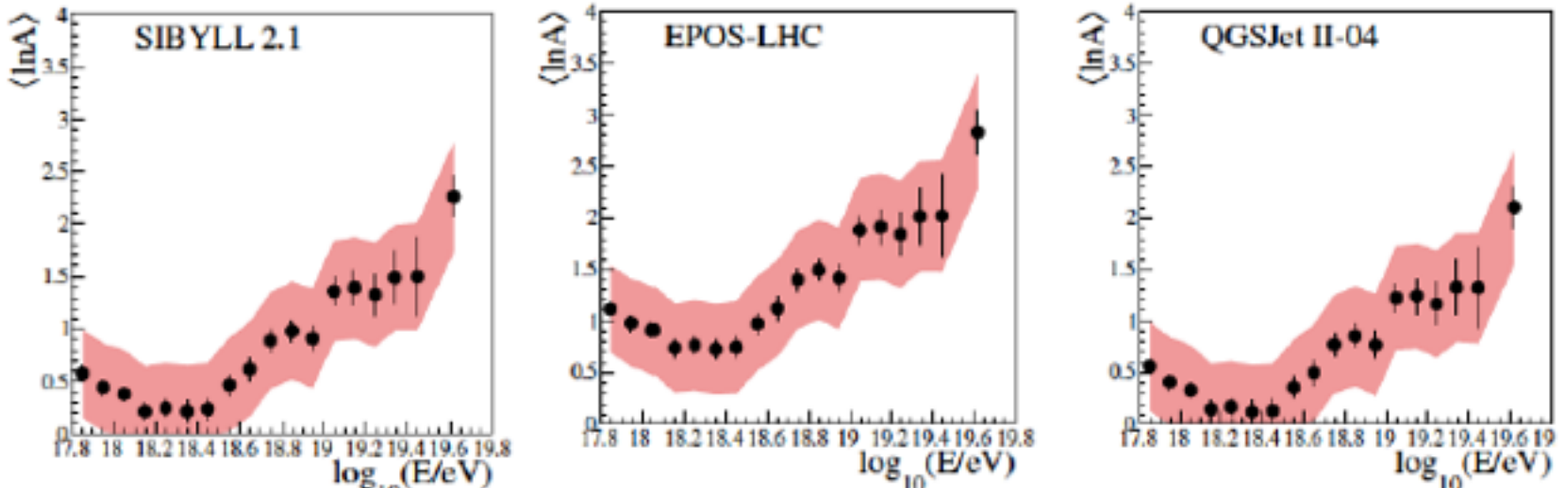

Average composition

<lnA> = 4 pure Fe

<lnA> ~ 2 50%Fe 50% p

<lnA>=0 pure p

σ(lnA)²

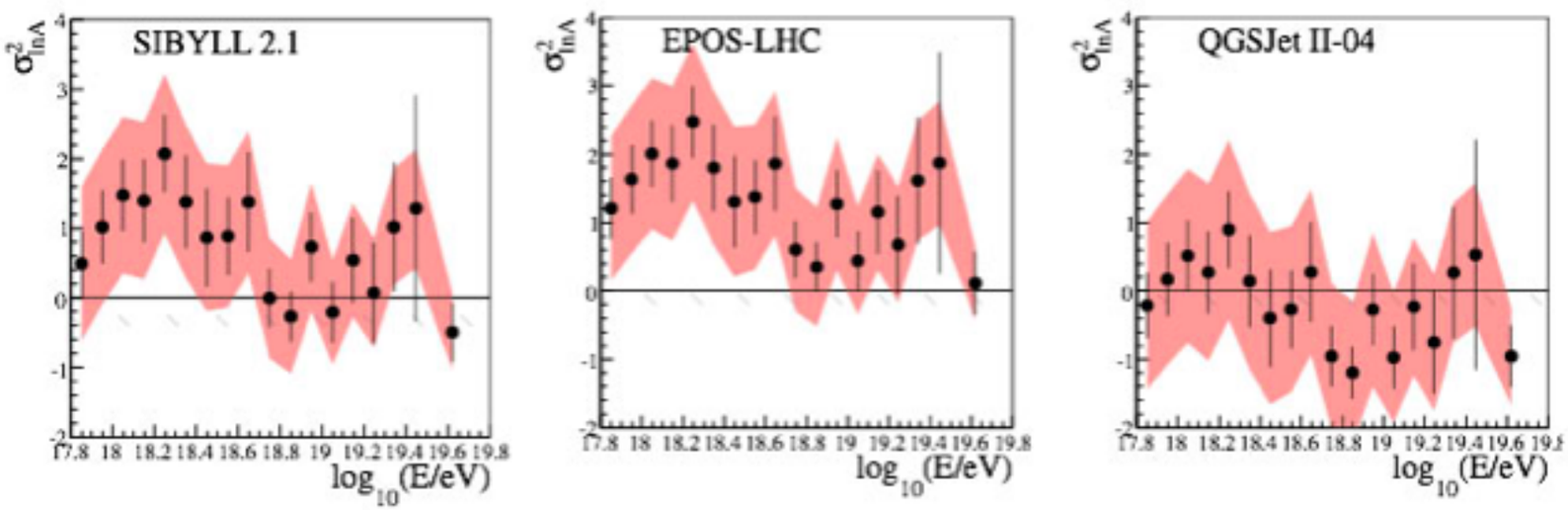

Dispersion of masses at ground
(source or propagation)

σ(lnA)=0 pure p or Fe

σ(lnA) ~ 4 50%Fe 50% p

- <ln A > minimum in ankle region
- Energy evolution common to all models <lnA> increasing from light to medium
- The mix include intermediates species

Mass Fraction from Xmax

Method: Fit in different energy bins the X_{max} profile from hybrid data with X_{max} profile from individual species (averaged shapes from MC)

Test of 3 models : EPOS-LHC , QGSJet II-4 and Sibyll 2.1

Example of profile fit for the E-range $10^{17.8}$- $10^{17.9}$ eV

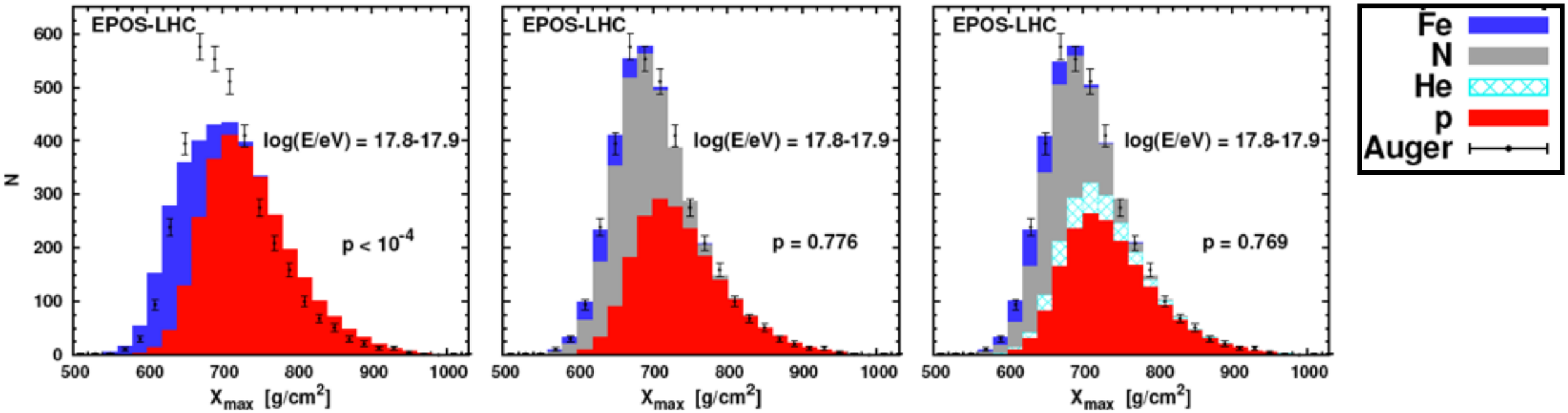

→ p-Value from maximum-likelihood fit

Mass Fraction from Xmax

Fitted fraction and quality : p and Fe only

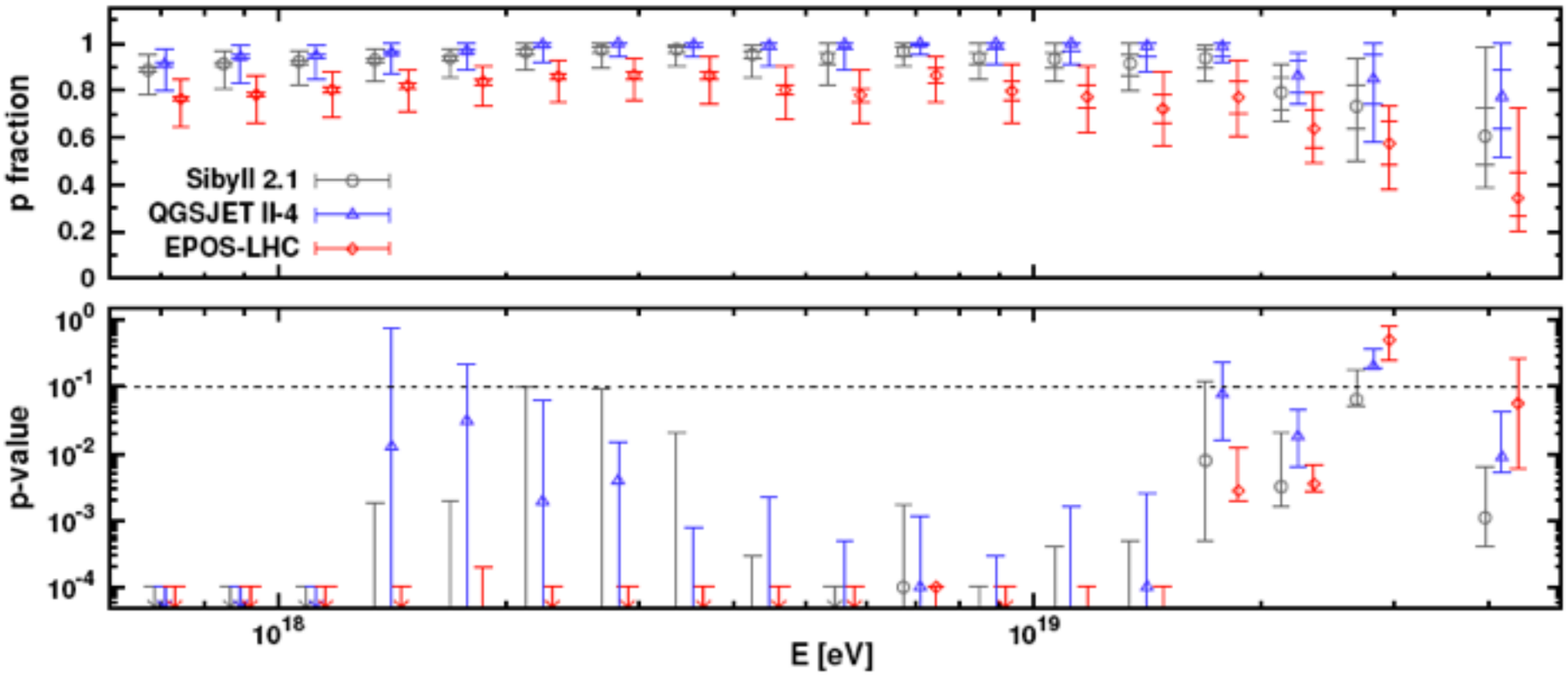

→ None of the models can reproduce the Xmax with p and Fe only

Mass Fraction from Xmax

Fitted fraction and quality with intermediate species: p, Fe, N and He

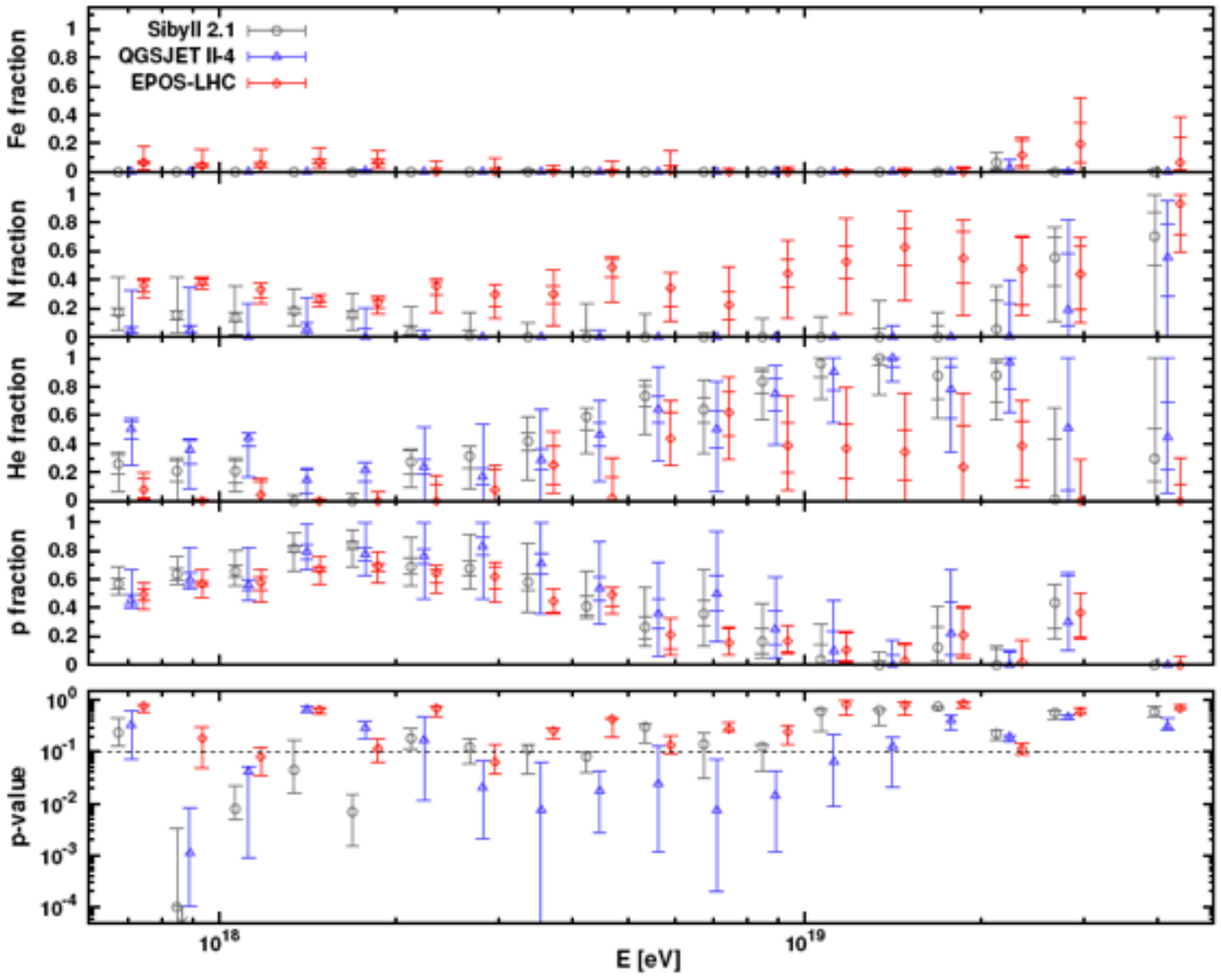

arXiv:1409.5083v1

Proton dominated composition is challenging hadronic models (even latest)

Mixed composition in agreement with EPOS-LHC in E-range

Statistics at high energy needed to check the trend ->need to use SD data

Mass composition from SD - MPD (Muon Production Depth)

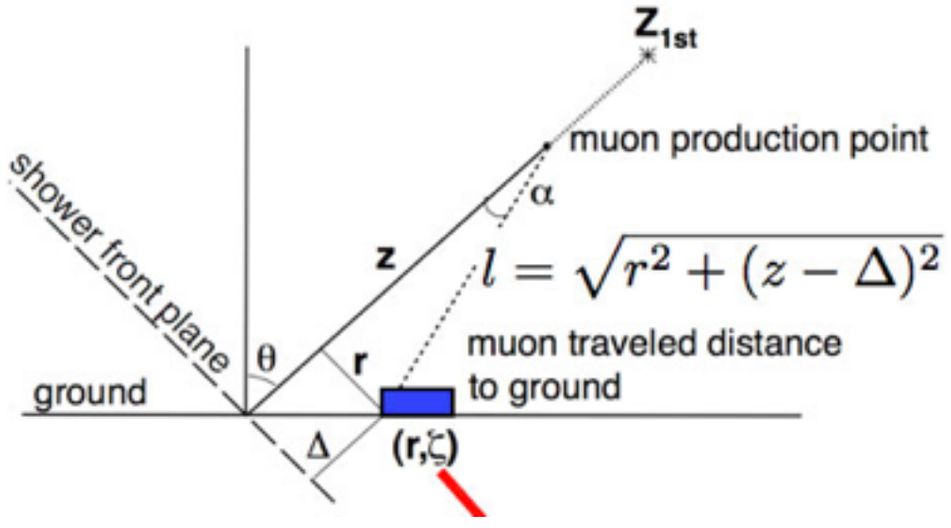

$$z = \frac{1}{2}\left(\frac{r^2}{ct_g} - ct_g\right) + \Delta$$

$$X^\mu = \int_z^\infty \rho(z')dz'$$

$$t_g \simeq t - < t_\varepsilon >$$

Data selection: θ>55 ° , traces from tanks between 1700 and 4000m only to avoid EM contamination

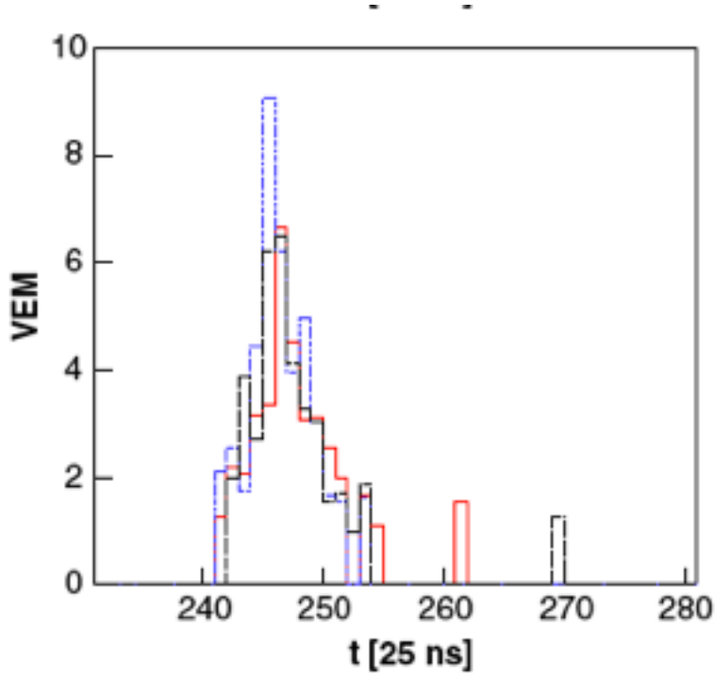

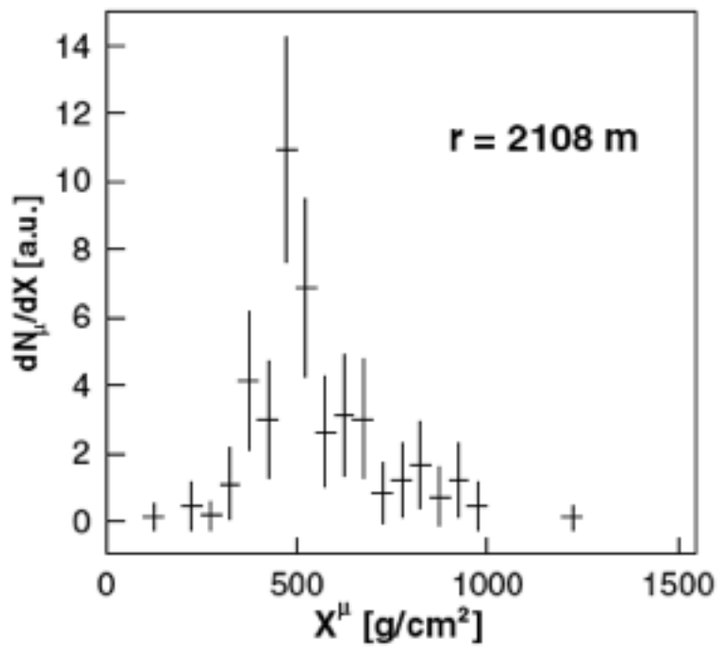

Mass composition from SD - MPD

Gaisser Hillas profile $\rightarrow X^{\mu}_{max}$

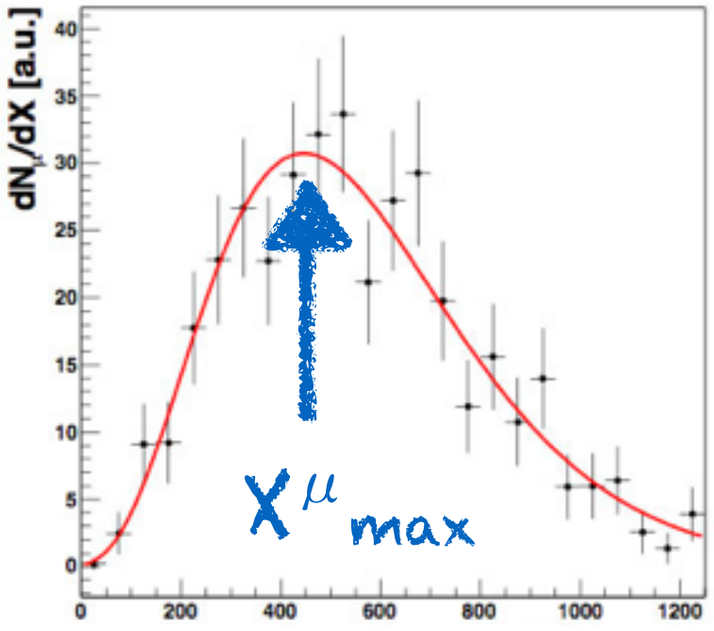

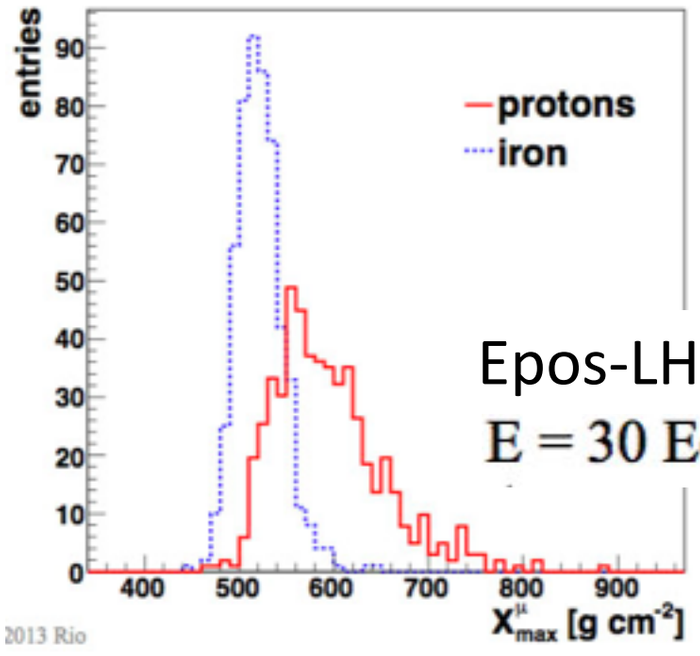

Epos-LHC

$E = 30$ EeV, $\theta = [55^o, 65^o]$

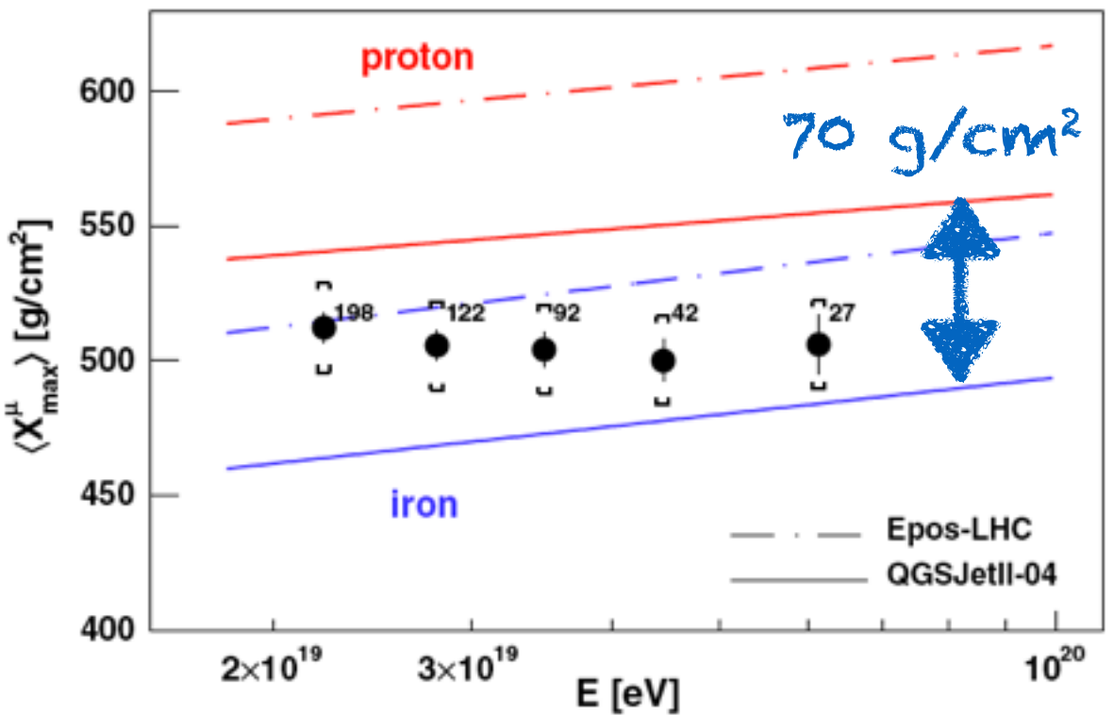

- Novel approach to study longitudinal profile
- Agree with conclusion of Xmax
  (but compatible with constant composition)
- Needs to be extended to more data
  (find methods to measure muons directly)

Interpreting X_{max} and X^{μ}_{max}

$$\langle \ln A \rangle = \ln 56 \frac{X^{p}_{max} - \langle X_{max} \rangle}{X^{p}_{max} - X^{Fe}_{max}}$$

$$\langle \ln A \rangle^{\mu} = \ln 56 \frac{X^{\mu p}_{max} - \langle X^{\mu}_{max} \rangle}{X^{\mu p}_{max} - X^{\mu Fe}_{max}}$$

lnA

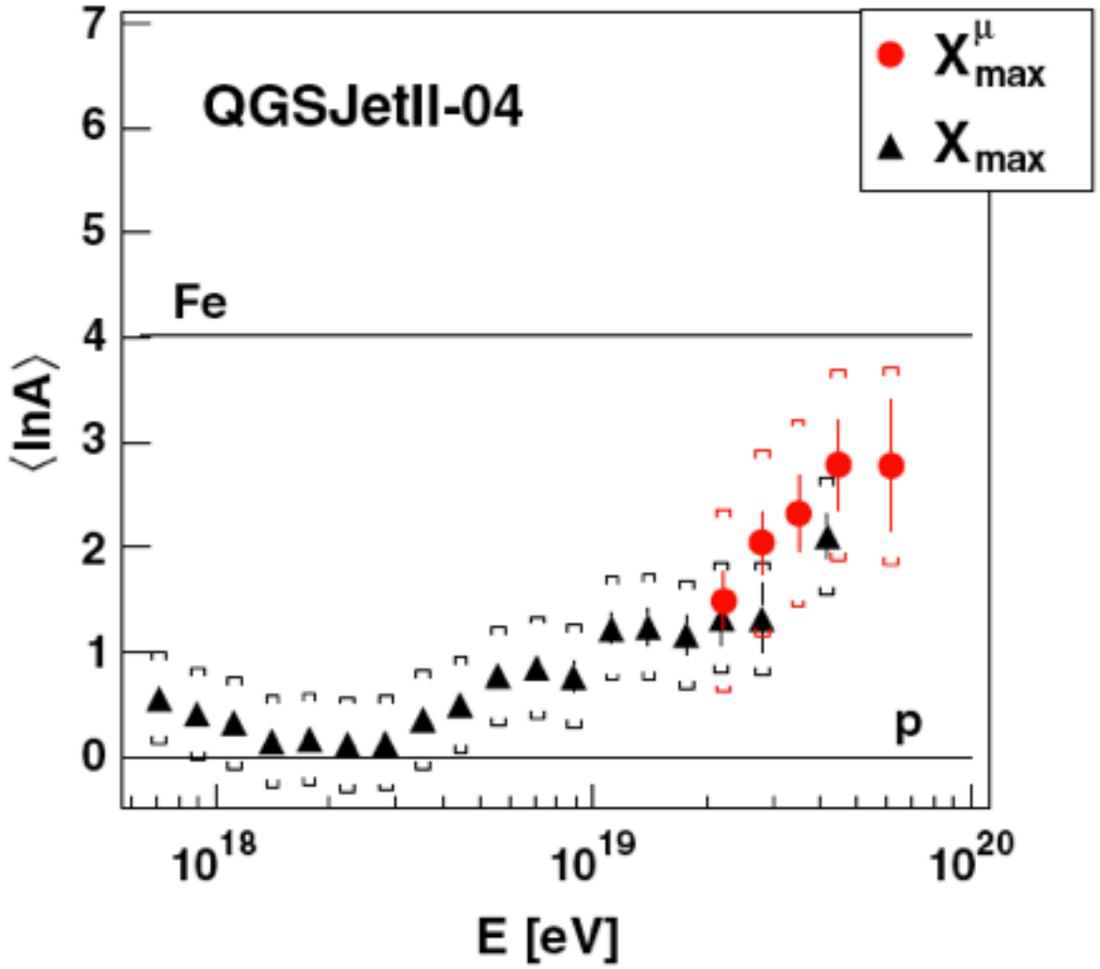

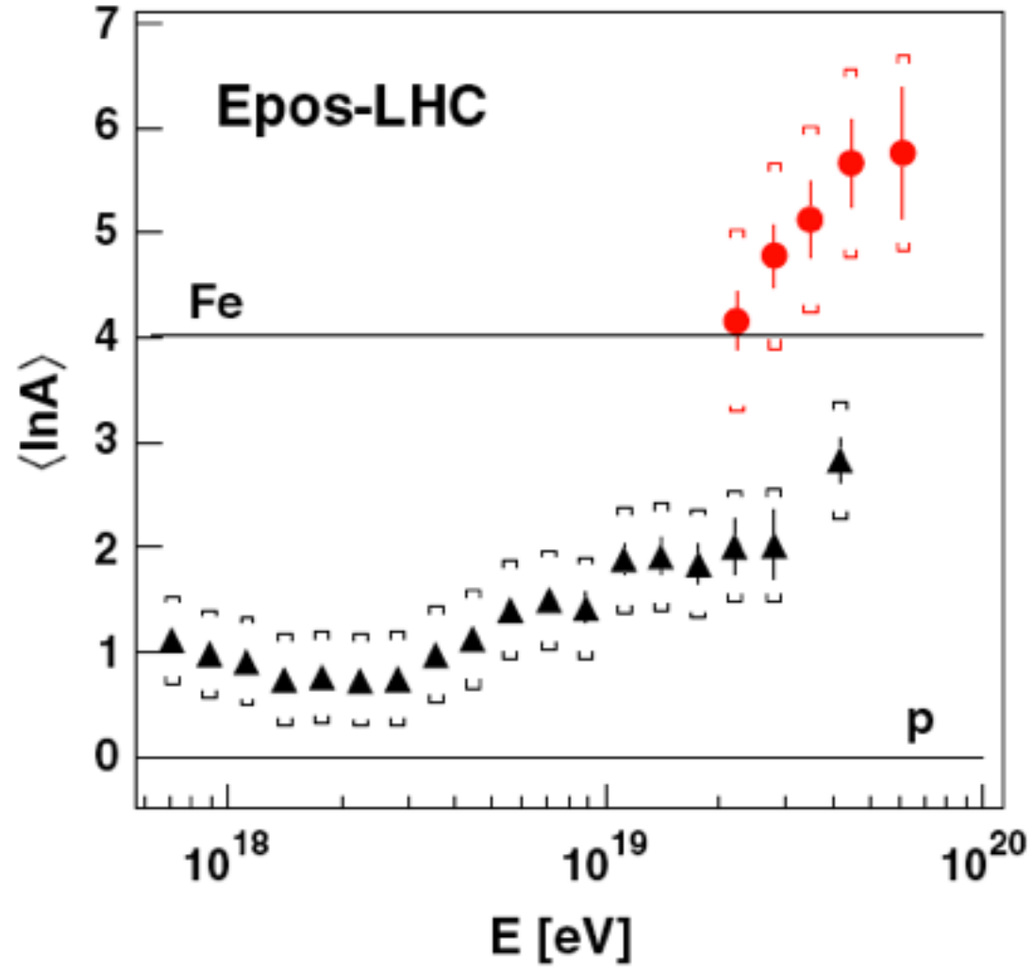

Phys Rev D90(2014)012012

Data are not consistently reproduced by models

Muon deficit in inclined showers

Rμ is N_{19}, the estimated number of muons, corrected from hadronic model dependency (<3%)

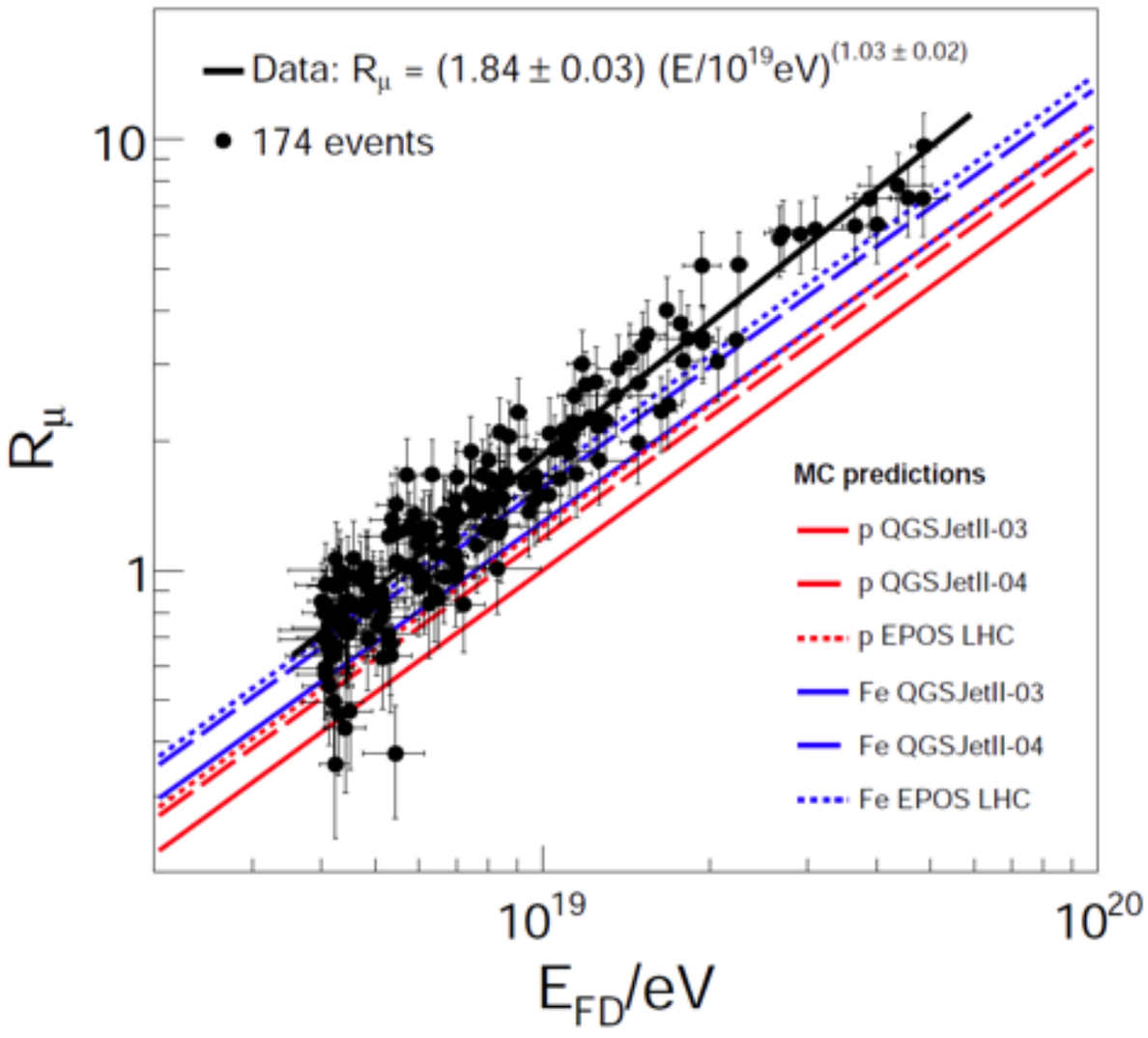

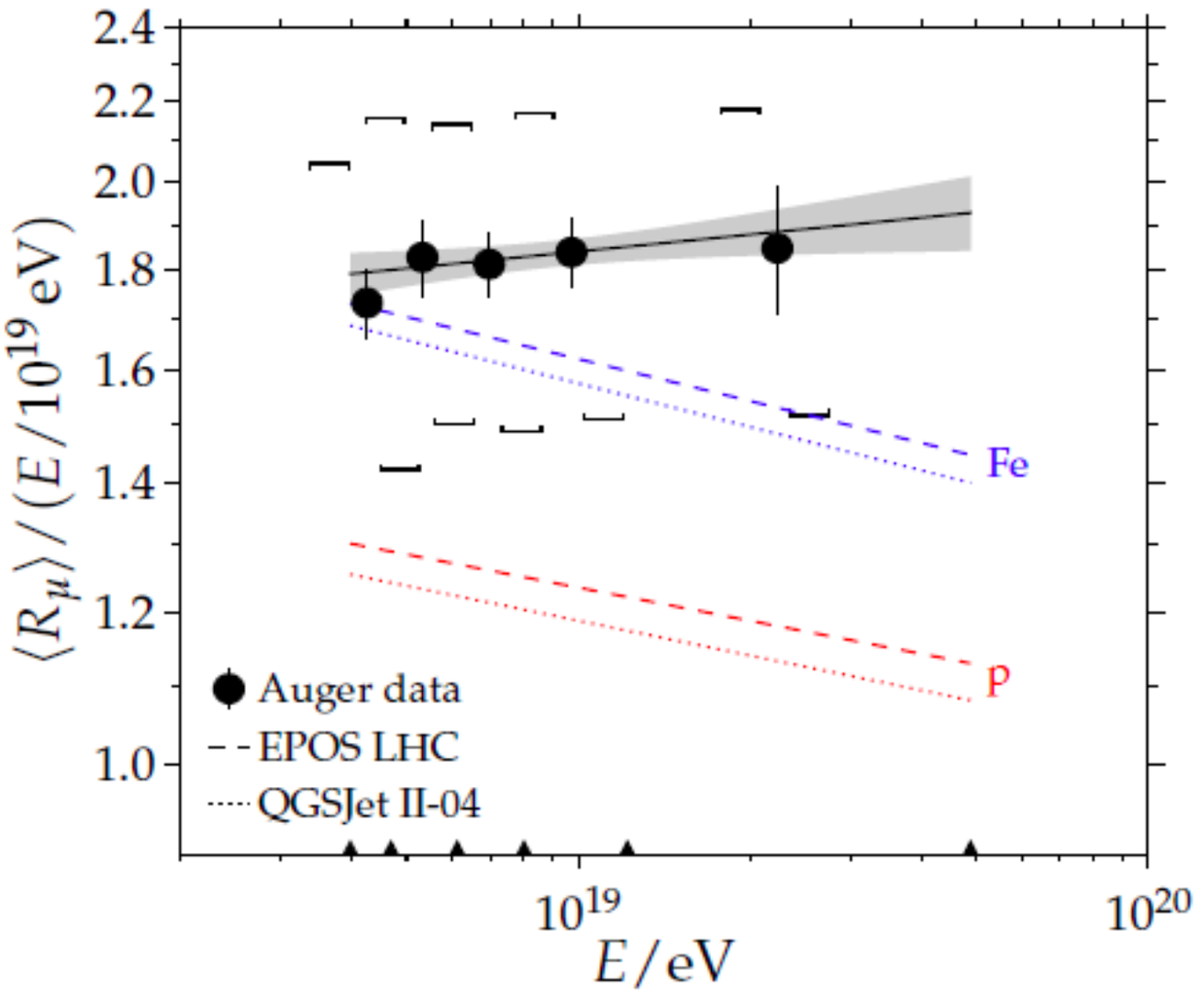

Muon numbers predicted by models are under-estimated by 30 to 80% (20%systematic)

arXiv:1408.1421v2

ANISOTROPIES

Anisotropy searches

Motivation: structure in the distribution of arrival directions may help to understand the nature and origin of UHECRs

Large scale anisotropies:

- Could signal galactic-extragalactic transition
- **Galactic:** diffusion & escape of galactic CRs below EeV energies might generate dipole pattern → Amplitude model-dependent, below few %.
- **Extragalactic:** diffusion in XG magnetic field and dipolar inhomogeneity of the nearby sources distribution. Small dipole due to our motion (Compton-Getting effect, expected below 1%).

Point sources anisotropies:

- Largest energies: above GZK a light composition component would arrive with small deflection from the source → trace source population

Large scale anisotropies

Method: Modified raleigh or east-west analysis on 1500 m and 750 m arrays dataset

Dipole Amplitude

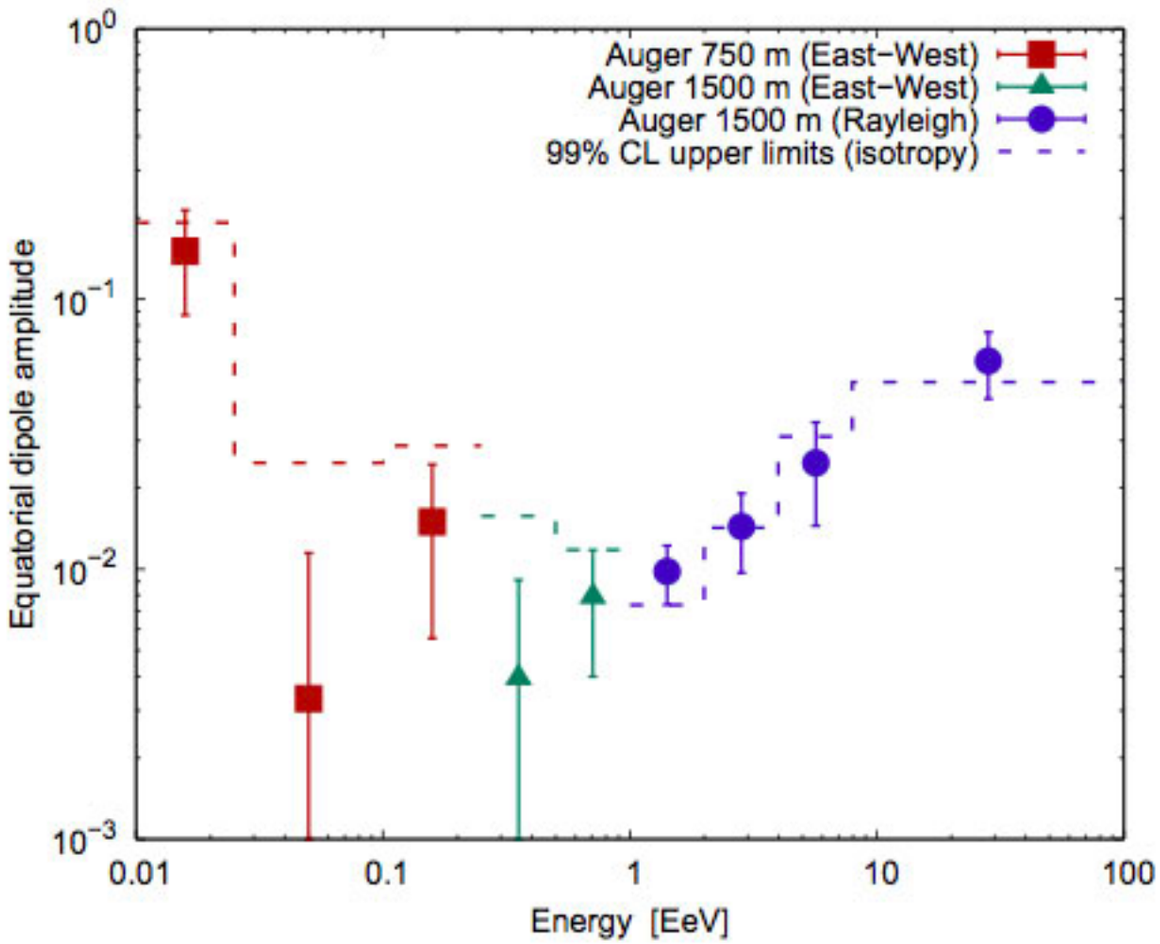

Dipole phase

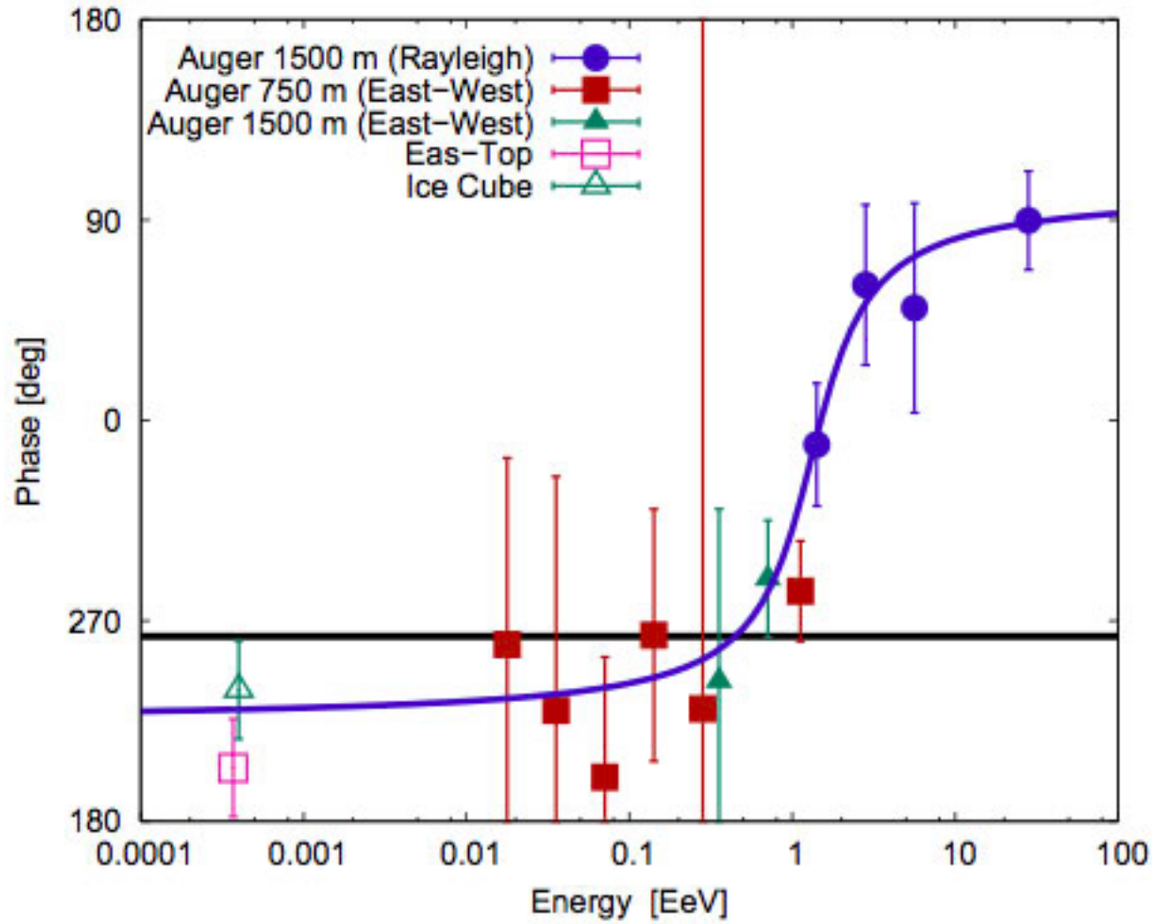

No evidence of anisotropy is found from amplitude

Hint for a smooth transition in phase from 270 ° below 1 EeV (Galactic origin?) to 90 ° above 4 EeV

Prescription running to eventually confirm

Point sources search

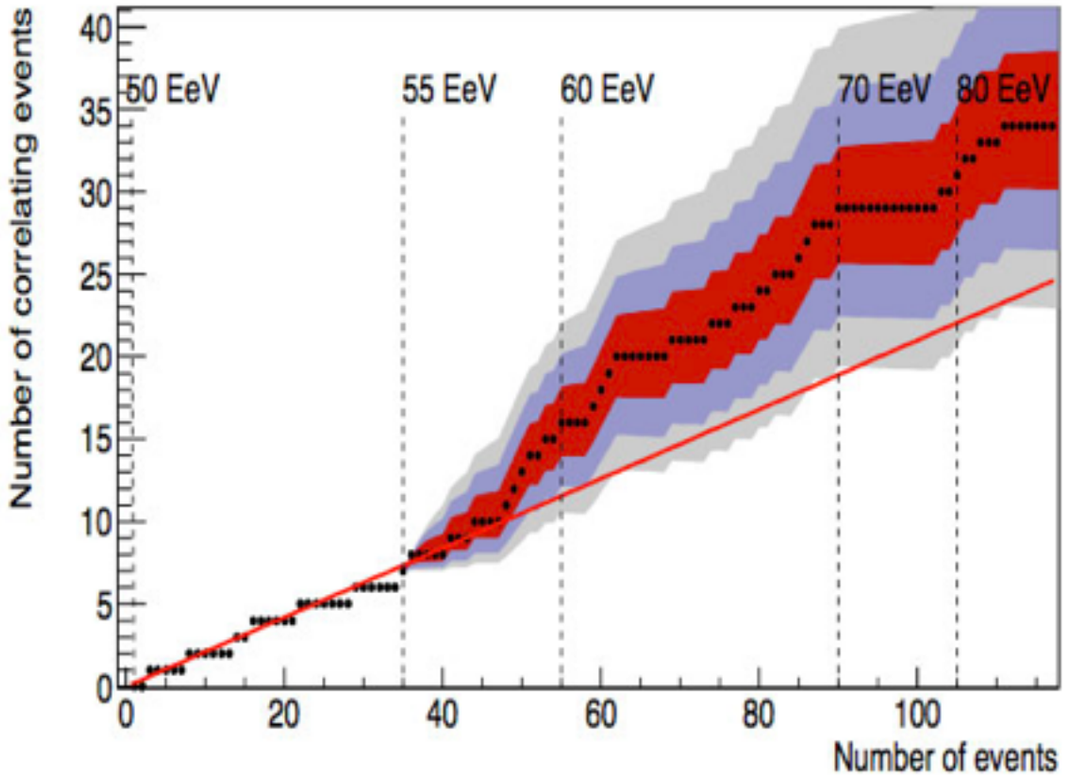

VCV catalog

Fraction of correlating events (33 ± 5) %

the content in protons at UHE is small :

consistency with Xmax

Centaurus-A

- Excess of events from a region close to CenA (l=-50.5o, b=19.4o)
- 19 events in a 240 circular window vs 7.6 expected
- KS test: max departure from isotropy ≥ that of observed events only in 4% of isotropic realizations

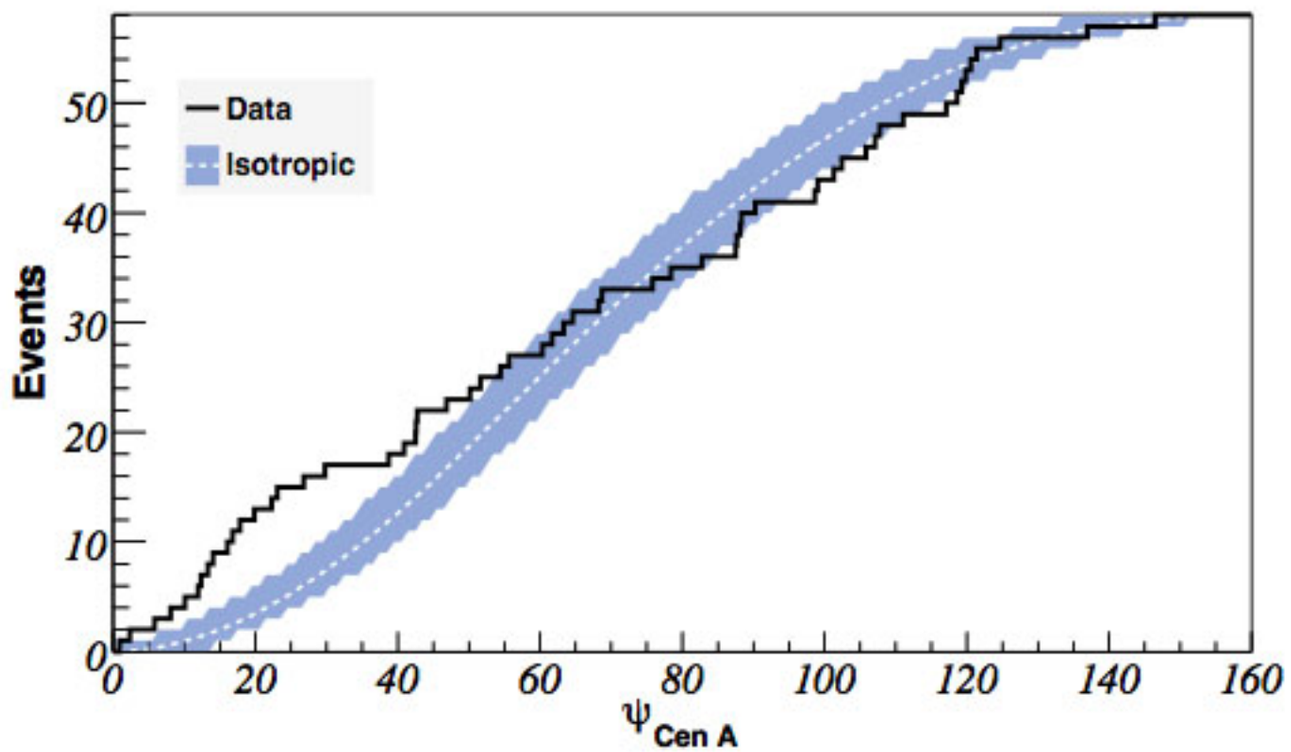

What did we learn with Auger ?

Spectrum

The ankle is clearly seen at $10^{18.72}$ eV

The cut-off is established (>20σ), E1/2 = $10^{19.63}$ eV !

What is the origin of the cut-off ? (Emax or GZK?)

What about the ankle ?

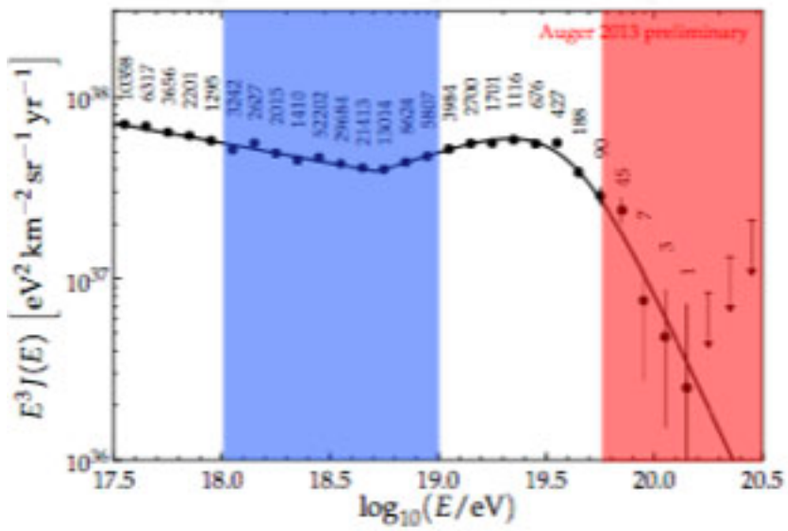

Composition

No primary photons: exclusion of top-down models

No photons/neutrons from Galactic sources

The composition gets heavier for increasing energy

Are there galactic proton at the ankle ??

Is there a proton component at the highest energies ? (10%)

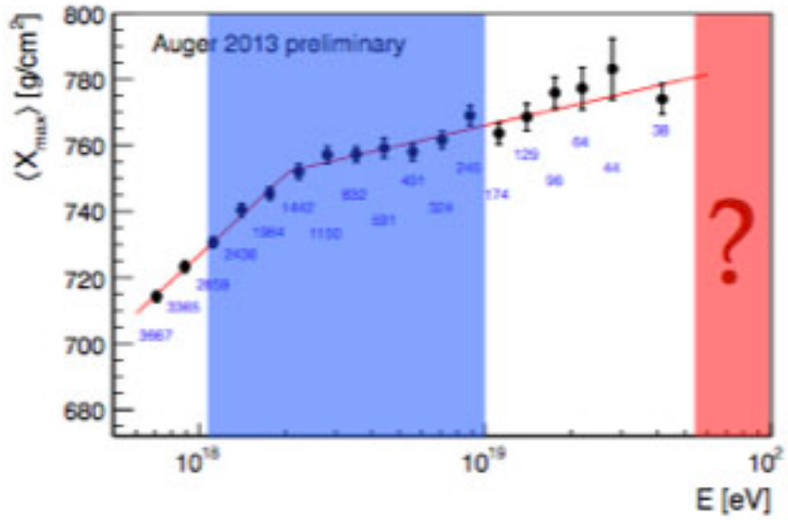

Anisotropies

No LSA above 1-2%

Hints for Gal-XGal transition from dipole phase ?

Point source anisotropy above 55 EeV (3σ level)

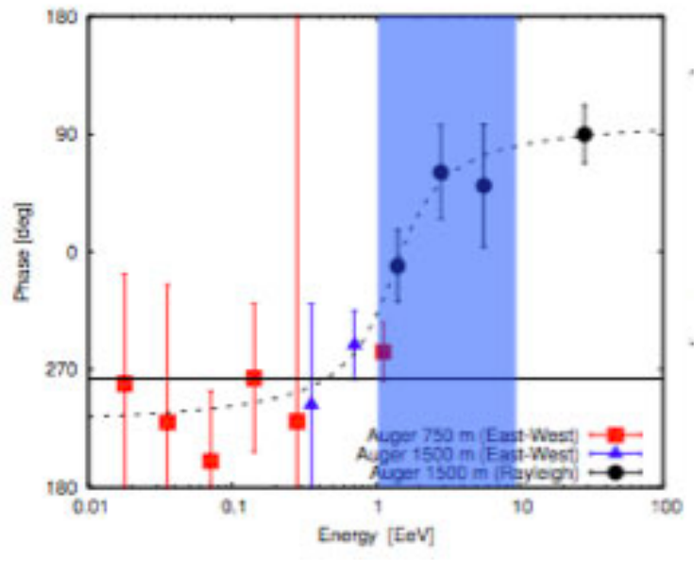

Hadronic physics

Muons put constraints to the hadronic interaction models

Science case for upgrading Auger Beyond 2015

- Origin of the cut-off (Emax or GZK)
- Proton fraction at the highest energies ? (->proton astronomy)
- Galactic/extra galactic origin , transition at the ankle?
- hadronic physics : particle physics beyond accelerators ?
- need to disentangle composition and hadronic interactions systematics

Improved composition estimators with high statistics needed !!

AUGER UPGRADE

Operate Auger until 2023 with improved detector composition sensitivity through **MUONS/EM** discrimination with the **Surface Detector**

SUMMARY

- The Pierre Auger Observatory has provided wealthy data of unprecedented quality
- Hard work to improve detector capabilities and give definitive answers to open key questions.
- Fruitful collaboration going on with TA

Thank you

BACKUP SLIDES

RECONSTRUCTION OF THE SHOWER PARAMETER, N_{19}

N_{19} : relative number of muons at ground wrt the density of muons of the reference distribution:

$$\rho_\mu = N_{19}\rho_{\mu,19}(x, y, \theta, \phi)$$

$\rho_{\mu,19}$: reference profile from parameterisation of muon density at ground of proton showers of 10^{19} eV simulated with QGSJetII-03 interaction model.

ρ_μ : model prediction for muon density at ground used to fit the signals recorded at the detectors.

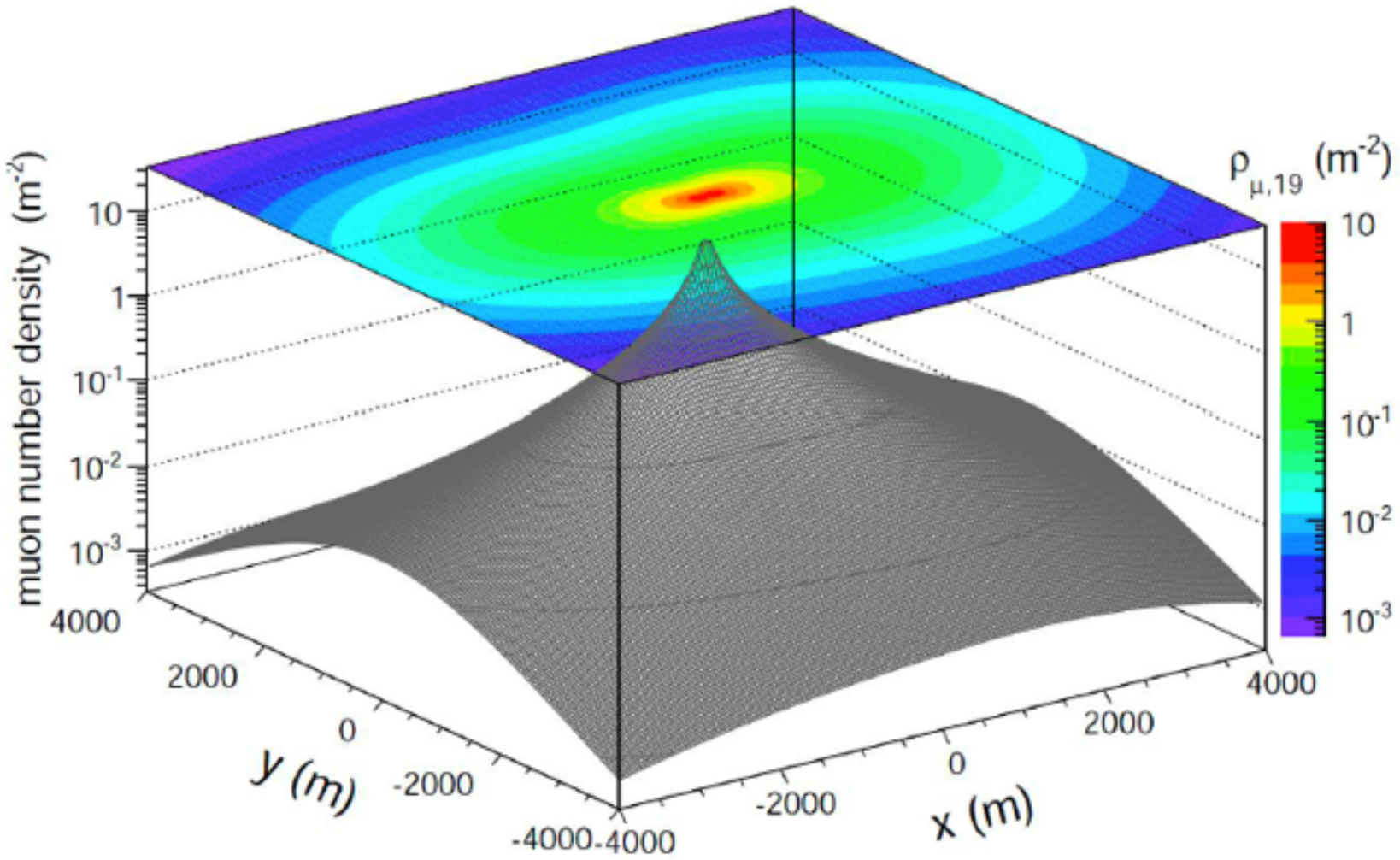

Example of $\rho_{\mu,19}$ for proton showers at θ=80°, ϕ=0° and core at (x,y) = (0,0)

ATMOSPHERE

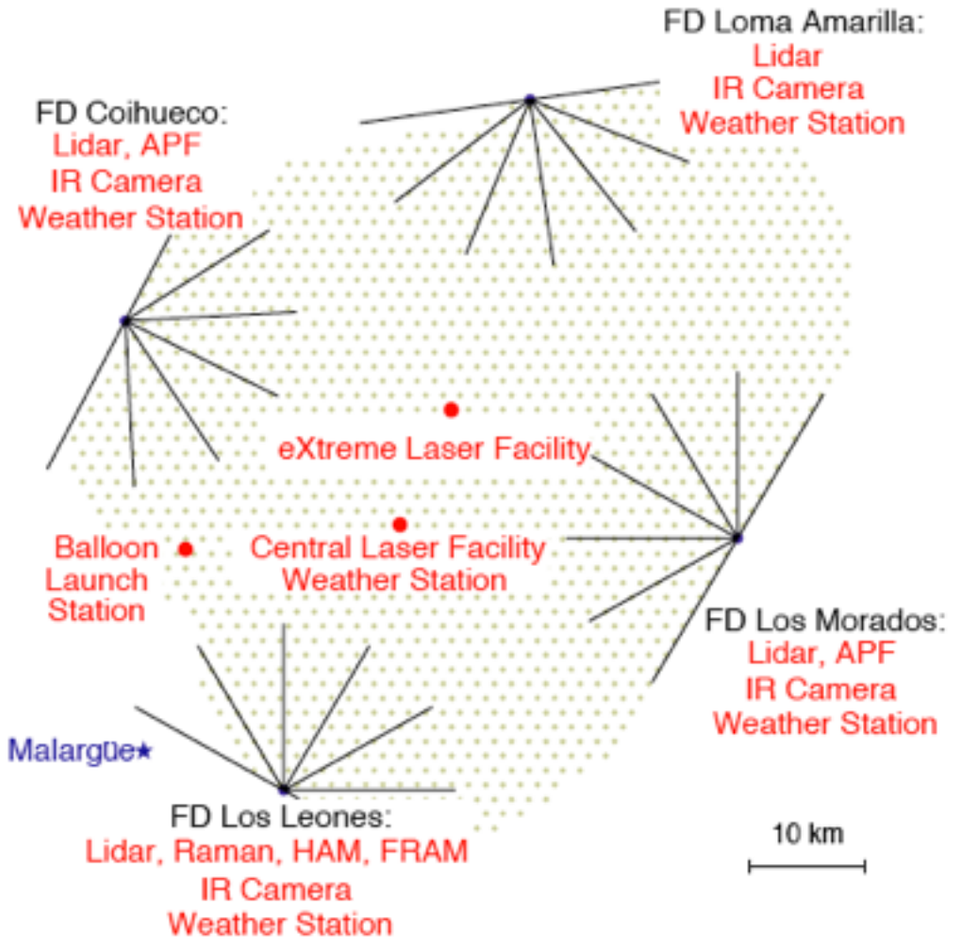

The Pierre Auger Collaboration
Astropart. Phys. **33** (2010) 108
Astropart. Phys. **35** (2012) 591

Production and transmission of the light (aerosols and molecular scattering)

Update of the hourly aerosol optical depth profiles measured with the laser facilities

distinction between correlated and uncorrelated uncertainties

L. Valore ICRC #0920

ΔE/E ranges from 3% to 6% for both types of uncertainty

FLUORESCENCE YIELD

Update of the absolute intensity of the 337 nm band (absolute normalisation of the wavelength spectrum)

Now AIRFLY: 4% uncertainty
M. Ave et al.,
Astropart. Phys. **42** (2013) 90

Before: 14% uncertainty
M. Nagano et al.,
Astropart. Phys. **22** (2004) 235

E lowered by 8%

ΔE/E ≈ 3.4%
(before we had 14%)

M. Ave et al., Astropart. Phys. **28** (2007) 41

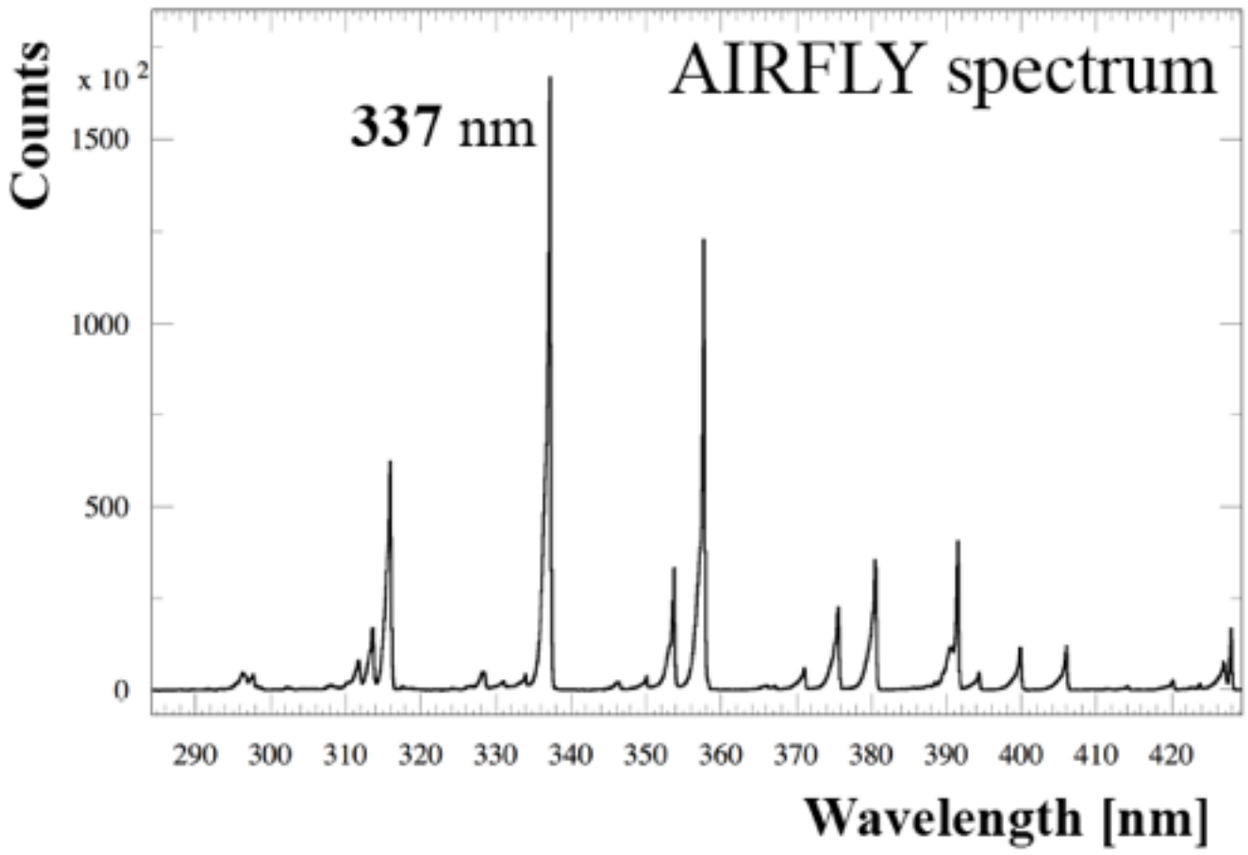

LONGITUDINAL PROFILE RECONSTRUCTION

Light collection: select pixels close to the image of the shower axis to maximise the signal to noise ratio

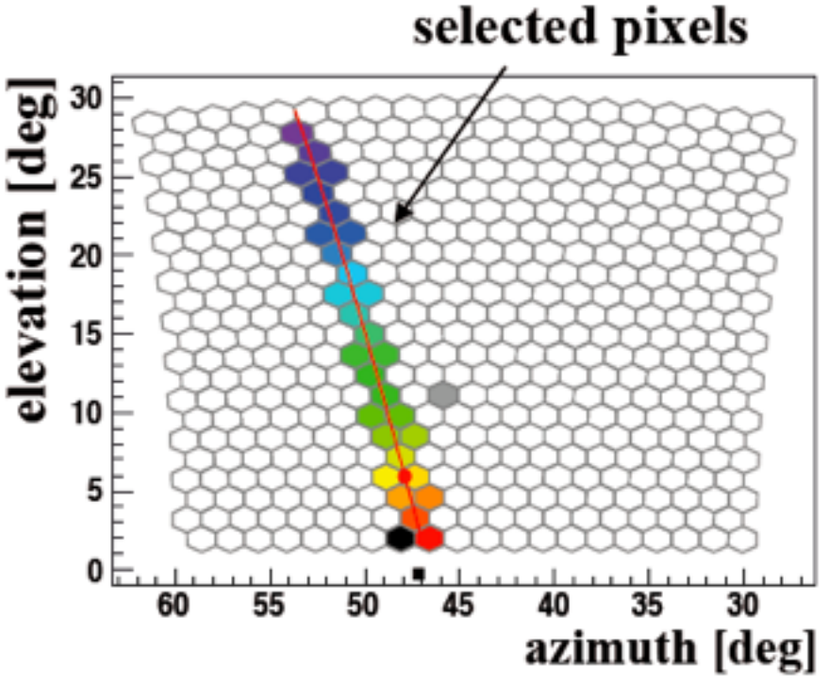

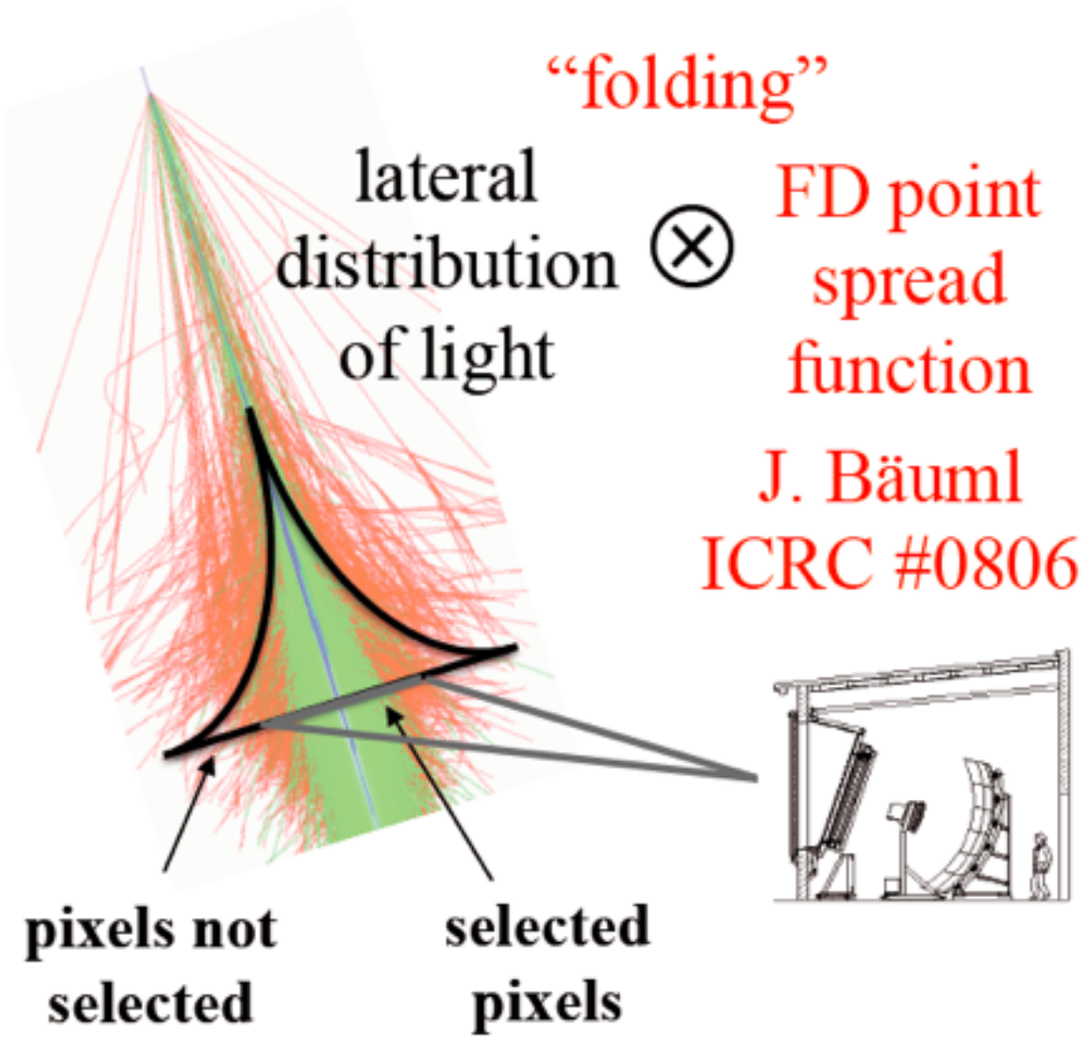

"folding"

lateral distribution of light ⊗ FD point spread function

J. Bäuml ICRC #0806

Correction for the light detected by not selected pixels:

- models for lateral distribution of fluorescence and Cherenkov light

- update of the reconstruction with a parameterisation of the "folding" from shower data:

E increased by 5% to 9%

$\Delta E/E \approx 5\ \%$

Radio detection in Auger (in MHz and GHz range)

AMBER

AERA

124 stations, 6km^2

EASIER

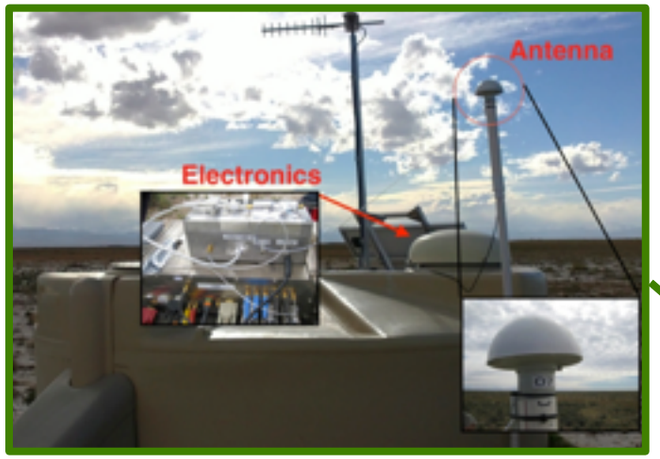

61 stations, 100 km^2

AERA

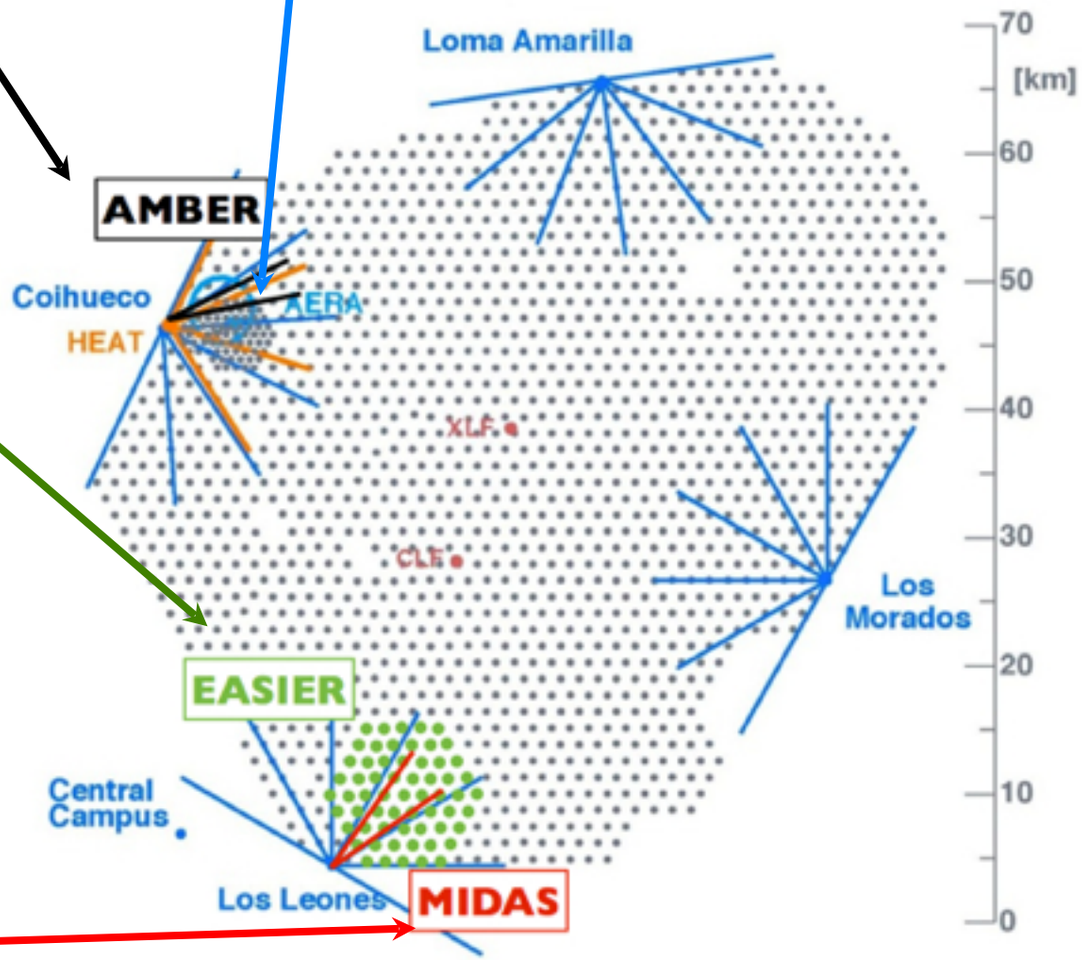

INVISIBLE ENERGY

Now estimated from Auger data M. Tueros ICRC #0705

Previously from simulation H. M. J. Barbosa et al., Astropart. Phys. **22** (2004) 159

➡ **reduction of the dependence on the hadronic interaction models and mass composition**

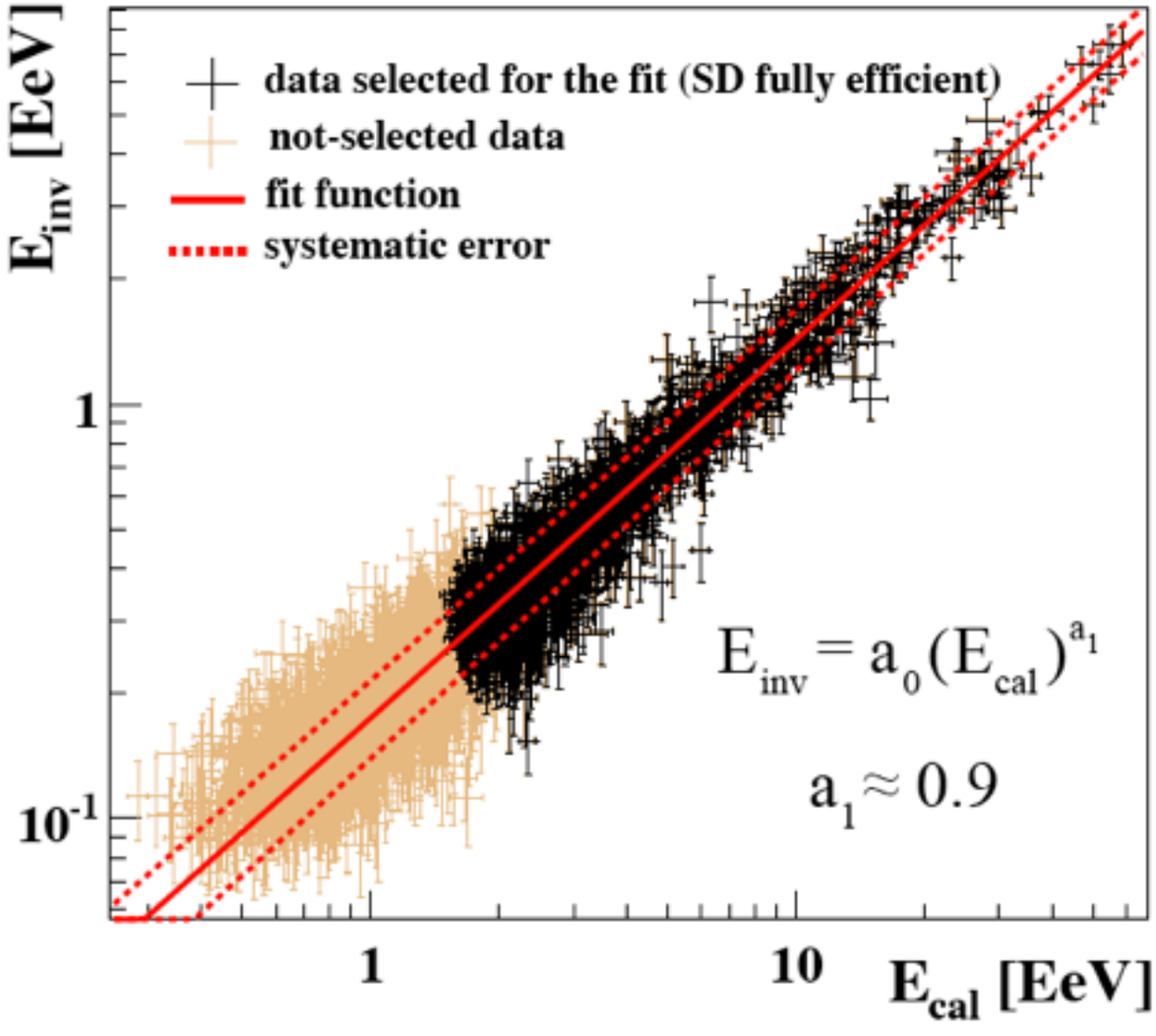

E_{inv} from SD signal and parameterised with an analytical function of the calorimetric energy (E_{cal})

$E_{inv} / E = 15\% \div 10\%$
lower at the higher energies

E increased by 4%

ΔE/E < 3 %

7

FD CALIBRATION

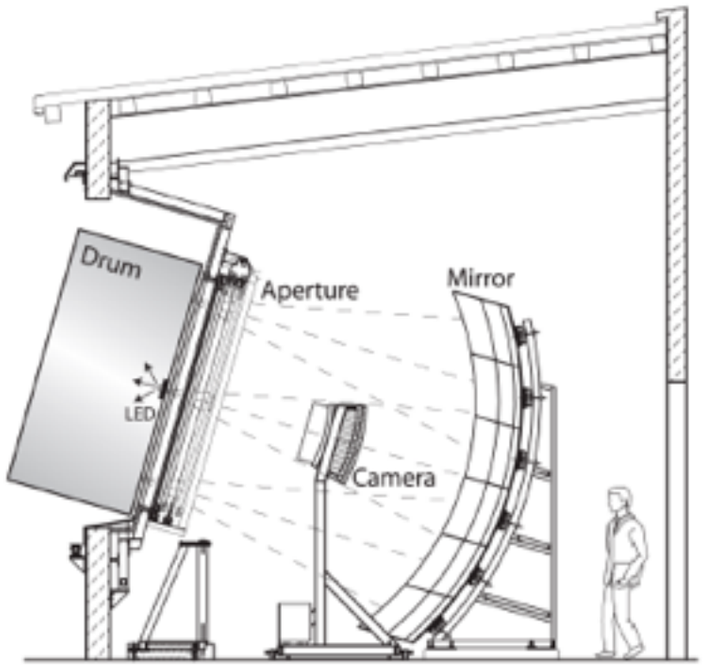

Drum
end-to-end absolute calibration at 375 nm

update to account for an optical *halo* caused by photomultiplier reflectivity

J. Bäuml ICRC #0806

E increased by 3%

$\Delta E/E \approx 9\%$ working to reduce at 5% level

J. T. Brack et al., JINST **8** (2013) 5014

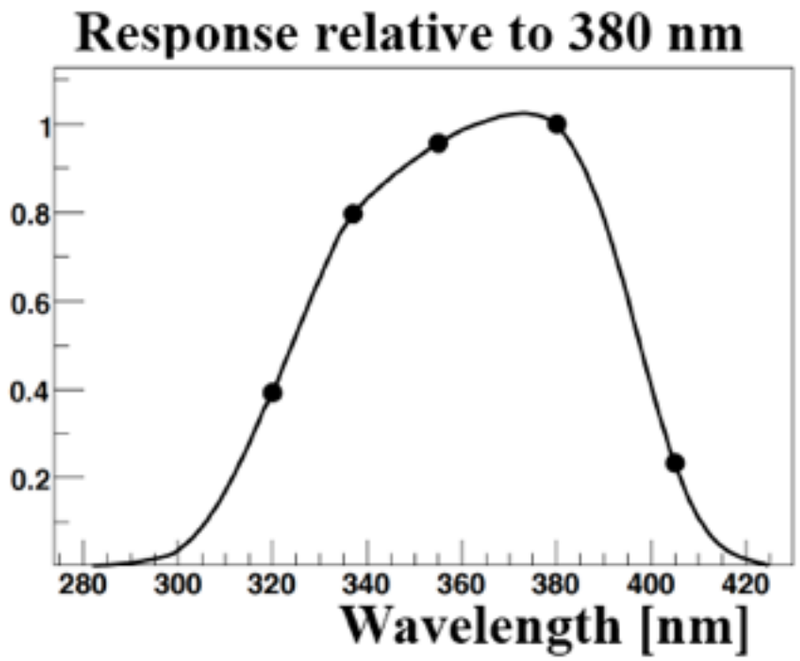

Relative optical efficiency

update based on drum multi-wavelength measurements

E increased by 4% **$\Delta E/E \approx 3.5\%$**